The Implications of Gauging Lepton Flavour Symmetries for Neutrino Masses and Dark Matter

By

RYAN PLESTID

Department of Physics and Astronomy
MCMASTER UNIVERSITY

A dissertation submitted to McMaster University in accordance with the requirements of the degree of MASTER OF SCIENCE in the Faculty of Science.

JULY 2015

Lay Abstract

In this thesis we examine the implications of adding a new force carrying gauge boson to the Standard Model in the presence of right-handed neutrinos.

This boson represents a new force that only affects leptons who belong to either the tauon or muon generation. We examine if one could explain neutrino masses and dark matter within the same theory by employing a Dodelson-Widrow like dark matter progenitor scenario suggested by Shuve and Yavin.

The compatibility of this scenario with neutrino oscillation data is discussed.

Abstract

The Standard Model of particle physics is a phenomenologically successful description of the strong, weak, and electromagnetic interactions at all currently accessible energy scales with few exceptions [1]. The notable deficiencies of the Standard Model are its inability to explain the matter anti-matter asymmetry, the existence of neutrino oscillations [2, 3], the anomalous magnetic moment of the muon [4, 5], and its failure to provide a suitable candidate for the gravitationally observed dark matter [6].

We explore an extension of the Standard Model that introduces a new gauge symmetry $L_\mu - L_\tau$ along with three right-handed neutrinos, and a symmetry breaking scalar field. The inclusion of right-handed neutrinos are motivated by the aforementioned neutrino oscillation data while the scalar field is motivated by cosmological bounds on a new Z'.

We attempt to fit our model to the observed neutrino mass textures in the see-saw limit. Despite having a Lagrangian density with three Yukawa

couplings, and four right-handed mass parameters we found the left handed neutrino mass matrix was controlled by only four independent quantities. We were attempting to fit to a set of five measured parameters $\{\Delta m^2_{12}, \Delta m^2_{13}, \theta_{12}, \theta_{23}, \theta_{13}\}$. This was found to be impossible with our proposed model. Higher dimensional operators were introduced to allow the model to generate neutrino textures that agree with experiment.

Our first minimal model was able to reproduce the correct neutrino textures with the exception of one of either θ_{13} or θ_{12} the disagreements was at the level of 25%. We found that our model was able to fit to the central value of neutrino data after the introduction of various combinations of dimension-five operators. The parametric dependence of these solutions were found to be incompatible with the Z' as a progenitor of dark matter scenario proposed by Shuve and Yavin [7]. The Z' progenitor scenario and the see-saw mechanism seem to be distinct entities in the sense that for the former to be viable the dark matter candidate cannot play a significant role in the generation of neutrino textures.

DEDICATION

This thesis is dedicated to my Oma who valued only my happiness above my education

ACKNOWLEDGEMENTS

I would like to first acknowledge both Brian Shuve and Itay Yavin for their assistance with this thesis particularly Chapter 5. I would also like to thank Itay for his patience and long discussions. I would additionally like to thank Brian Shuve for all of the time he has committed to teaching me and for his constant availability. I would also like to thank Sung-Sik Lee for his willingness to discuss questions of mine and for making problems transparent that were previously opaque. I would like to acknowledge Shouvik Sur and Sedigh Ghamari for their helpful conversations when I was first learning field theory and subsequently for their ability to help me think about field theory beyond the scope of particle physics. Finally I would like to thank my parents, my siblings, my Oma and Leanne for always supporting me and encouraging me to pursue my dreams.

AUTHOR'S DECLARATION

I declare that the work in this dissertation was carried out in accordance with the requirements of the University's Regulations and Code of Practice for Research Degree Programmes and that it has not been submitted for any other academic award. Except where indicated by specific reference in the text, the work is the candidate's own work. Work done in collaboration with, or with the assistance of, others, is indicated as such. Any views expressed in the dissertation are those of the author.

SIGNED: ..... DATE: .....

TABLE OF CONTENTS

Page

List of Tables **xv**

List of Figures **xvii**

1 Introduction **1**

1.1 Effective Field Theory 3

1.2 Accidental Symmetries of the Standard Model 9

1.3 Anomalous Symmetries 13

1.4 Neutrino Oscillations 16

1.4.1 PMNS Matrix 18

1.4.2 Mixing Data 19

1.4.3 See-Saw Mechanism 20

1.5 Dark Matter 22

1.6 Sterile Neutrinos as Dark Matter 27

2 Overview of the Proposed Model **35**

2.1 Phases of Parameters 37

2.2 Consequences of Singlet Symmetry Breaking 39
2.2.1 A Massive Z' 39
2.2.2 Contributions to the Neutrino Mass Matrix 42
2.2.3 Singlet Field in the Broken Phase 44
2.3 The Z' Progenitor Scenario Proposed by Shuve and Yavin 2014 45
2.3.1 Restrictions on a new Z' 47
2.4 Dark Matter Candidates in Our Model 51

3 Fitting To Neutrino Data 55
3.1 Mass Matrix Parameterization 56
3.2 Generation of Possible Mass Matrices 58
3.3 Successes of this Minimal Model 61

4 Modifying the Model 65
4.1 Possible Dimension-Five Operators 66
4.2 Consequences of Mass-Inducing Operators 68
4.2.1 Finding the Model Parameters 70
4.3 Yukawa-Inducing Operators 72
4.3.1 Motivation 72
4.3.2 Resultant Left-Handed Mass Matrix 74
4.4 Weinberg-Inducing Operators 76
4.5 A Comment on the Mass Scale 77
4.6 A Quick Summary 79

5 Dark Matter Viability and X-ray Constraints **81**

5.1 Mixing angles in the See-Saw Limit 82

5.2 Requirements for Z' Progenitor Dark Matter 83

5.3 A Single-Sterile Effective Theory 84

5.3.1 Zeroth-Order Result 86

5.3.2 First-Order Corrections to the Eigenstates 87

5.3.3 Second-Order Corrections to the Eigenvalues 88

5.3.4 Integrating out the Super Massive Sterile States . . . 88

5.4 Mass-Inducing Operator Parametrics 91

5.5 Yukawa-Inducing Operator Parametrics 94

5.6 Both Yukawa- and Mass-Inducing Operators 96

6 Conclusions and Future Directions **101**

A A Brief Review of the Higgs Mechanism in the Context of the Standard Model **107**

B Method for Extracting Lagrangian Parameters **113**

B.1 Generating the Correct Mass Spectra 114

B.2 Re-expressing in the Flavour Basis 115

B.3 Strategy to find Candidates for our Theory 116

B.4 Extracting Lagrangian Parameters 117

Bibliography **119**

List of Tables

Table **Page**

1.1 Data from nu-Fit after fitting to global data from 'NOW' conference in 2014 [8]. This table is taken from the nu-Fit collaboration website (2015) 20

2.1 Charge assignments of the relevant fields under hypercharge $SU_W(2)$and the new $U'(1)$. Here 2 refers to the fundamental representation of $SU(2)$. 36

3.1 Comparison of minimal model's predicted neutrino texture for $r = 0.8212$, $\mu = -0.61$, $\mu_e = 0.75$. This texture is in the normal hierarchy and so $\sin^2\theta_{23}$ is the appropriate value. All neutrino data is taken from [8] 63

4.1 Parameter values for mass-inducing operators that fit to the data. $\frac{m_\ell}{m_2}$ is the ratio of the lightest mass to m_2 72

4.2 Parameter values for Yukawa-inducing operators that fit to the data. $\frac{m_\ell}{m_2}$ is the ratio of the lightest mass to m_2. 76

5.1 Parameter values for Yukawa-inducing operators and mass-inducing operators in a $y_e = 0$, $m_\mu = m_\tau = 0$ limit that fit to the data. $\frac{m_\ell}{m_2}$ is the ratio of the lightest mass to m_2. 98

A.1 Charge assignments of the fermionic and scalar fields in the Standard Model. The gauge bosons transform in the adjoint representation. The indices $m \in \{e, \mu, \tau\}$ and $n \in \{u, c, t\}$ denote the generations of leptons or quarks respectively (i.e. $d_c := s$ the strange quark). All fermionic fields are defined as left-handed Weyl spinors. The triplet representations under $SU_c(3)$ are indexed by colour while the first generation $SU_L(2)$ are defined in Equation A.1 the additional generations are obtained by trivial substitution. The nomenclature for groups is such that the number is the dimension of the representation while the bar differentiates between objects transforming as a tensor with upper indices (bar) v.s. with lower indices (no bar) (see Coleman Aspects of Symmetry [9]) 109

LIST OF FIGURES

FIGURE **Page**

1.1 The diagram on the left shows $\psi + \psi \rightarrow \psi + \psi$ scattering in the high energy theory mediated by the massive vector boson. The diagram on the right is the same process in the low energy theory where the scattering is mediated by the dimension-six operator parameterized by G_F 8

1.2 Leading order $\phi \rightarrow 3\psi$ decay process for the two charge assignment choices with the right diagram corresponding to 1.5(b) and the left diagram corresponding to 1.5(a) 12

1.3 Triangle diagrams used to calculate anomaly coefficient for gauge symmetries 15

1.4 A schematic diagram showing a freeze-out scenario. The dark matter species remains in equilibrium until some critical temperature and then it decouples from the photon bath resulting in a relic abundance. Figure taken from Hooper (2009) [10] 26

1.5 An example of a process that contributes to the production of a sterile neutrino abundance via transformation of an electron into an electron neutrino (written in flavour basis) which composes some small component of the mass eigenstate N. As a result there is a non-vanishing probability of "transforming" an electron into a sterile neutrino. 30

1.6 Primary decay mode for a heavy sterile neutrino $N \rightarrow \nu + \gamma$ via a loop process with a charged W boson and any Standard Model fermion charged under $SU_W(2)$ resulting in the emission of a neutrino and a photon. 31

1.7 Constraints on sterile neutrino dark matter from observations of the Milky Way [11]. Figure taken from Boyarsky *et. al.* (2006). . 33

2.1 Plot showing contours in the $g' - M_{Z'}$ plane that fit to various masses of the sterile neutrino in the Z' progenitor scenario [7]. This plot was taken from Shuve and Yavin (2014) 48

2.2 Z'contribution to the anomalous magnetic moment of the muon $(g-2)_\mu$ 49

2.3 Decay mode of a heavier sterile N_2 into Standard Model particles and the dark matter candidate N_1 via a Z' interaction 50

2.4 Bounds on a Z' coupling to the charge $L_\mu - L_\tau$ in the g' vs $M_{Z'}$ plane. Bounds from Borexino are sub-dominant to all other bounds. Neutrino trident production is the leading bound for $M_{Z'}$ larger than about 4 MeV. Plot produced by Brian Shuve. For a review of these bounds see ref. [12] 52

3.1 Possible normal hierarchy mass matrices' r_{22} and r_{33} generated by taking central fit values for the PMNS matrix [8] and rotating all possible mass spectra that conform to the data for the normal hierarchy into the flavour basis 61

3.2 Possible Inverted hierarchy mass matrices' r_{22} and r_{33} generated by taking central fit values for the PMNS matrix [8] and rotating all possible mass spectra that conform to the data for the inverted hierarchy into the flavour basis 62

4.1 Parton level diagram contributing to neutrinoless double beta decay. This diagram is written using two component spinor techniques where the arrows track chiral charge. We see that to get two outgoing electrons that couple to the weak charged-current we need a Majorana mass term M_{11}. 78

CHAPTER 1

INTRODUCTION

There are a variety of phenomenological problems present in the Standard Model. The three most pressing of these are the inability to explain the observed matter anti-matter asymmetry, the existence of neutrino masses, and the absence of a dark matter candidate. There also exist some discrepancies with Standard Model predictions whose significance is disputed. One example is the anomalous magnetic moment of the muon [5]. These issues signify that the Standard Model is not complete and requires additional matter content.

In the following research we will investigate a possible extension of the Standard Model that contains ingredients necessary to solve the latter three

problems. We investigate whether, in this extension, the parametrically viable regions to solve each of these discrepancies overlap.

In the Standard Model there are four accidental global symmetries that are conserved, these are the three generation lepton numbers and baryon number [13]. Certain combinations are gauge invariant and can be coupled to a new gauge field self consistently. One such combination is the difference between muon type lepton number and tauon type lepton number $L_\mu - L_\tau$.

Our theory begins by assuming that $L_\mu - L_\tau$ is the charge that couples to an, as of yet undiscovered, fifth fundamental force mediated by a spin-one boson; this is the Z'. If this is the case cosmological constraints on the mass of a Z' requires the gauge symmetry to be spontaneously broken [14]. We elect to use the Higgs mechanism and introduce a complex scalar field which transforms non-trivially under $U'(1) := U_{L_\mu - L_\tau}(1)$ and has some non vanishing vacuum expectation value that causes the symmetry to be realized non-linearly. It should be noted that for most of our work regarding the neutrino textures and dark matter production we remain fairly agnostic about the mass generating mechanism.

For the correct neutrino phenomenology to be realized one conventionally extends the Standard Model by assuming the existence of right handed neutrinos which are $SU(2)$ singlets. Unlike their left handed counterparts no gauge symmetry prohibits the existence of Majorana mass terms for these

gauge singlets and they will in general take the form of an unconstrained 3x3 matrix that couples the various generations to one another. In our proposed scenario the form of this mass matrix is restricted by our imposed $U'(1)$ symmetry and charge assignments. These restrictions are responsible for the difficulty in reproducing the observed phenomenology.

Additionally the existence of a heavy Z' can potentially give rise to a population of sterile neutrino dark matter via decay [7]. The purpose of this thesis is to analyze the compatibility of this scenario and the neutrino texture data.

In this thesis we provide a decisive answer to this question. In this chapter the necessary background information will be covered. In Chapter 2 we will present the model and cover it's basic features. In Chapter 3 the model's ability to produce neutrino textures that agree with experiment will be discussed. Chapter 4 will focus on sensible modifications to the model in the language of effective field theory. Chapter 5 will discuss the interplay between dark matter and neutrino masses.

1.1 Effective Field Theory

In a physical theory it is often the case that energetics dictate the possibility of exciting certain degrees of freedom within a system. For example electron positron pair production only becomes possible for centre of mass energies

above $2m_e = 1.022$ MeV . This creates a heirarchy of energy scales where different degrees of freedom become accessible. Organizing one's theory with respect to this hierarchy is computationally advantageous because one need only analyze the degrees of freedom which are relevant at the scale of interest [15]. In particle physics as one lowers the energy scale more and more degrees of freedom are "frozen out" due to the energy gap associated with massive particles. Once again pair production is a good example of this phenomenon. A concrete example of this phenomena is a toy model of the weak interaction with one fermion species ψ and a massive vector boson A_μ

$$\mathscr{L} = \overline{\psi}(i\partial\!\!\!/ - m)\psi - \frac{1}{4}F_{\mu\nu}F^{\mu\nu} + \frac{1}{2}M^2 A_\mu A^\mu - g\bar{\psi}A\!\!\!/\psi \tag{1.1}$$

with m the tree level mass of the fermion and M the tree level mass of the vector boson, where $M >> m$ and $F^{\mu\nu}$ is the field strength tensor and the action is given by $S := \int \mathrm{d}^4x\mathscr{L}$. The slashed notation denotes contraction with the four dimensional gamma matrices. For kinematic regimes in which the centre of mass energy of any two particles is less M, the vector boson can not be produced and ceases to be a propagating degree of freedom.

A natural question to ask is what are the implications of the existence of a super massive particle for the system at low energy given that it's interpretation as an asymptotic state can no longer be realized. We can analyze this question in the path integral picture as follows. The theory is

defined by the partition function given by

$$Z = \int \mathscr{D}\psi \mathscr{D}A e^{iS[\psi,A]} \tag{1.2}$$

however one can perform the path integral over some subset of field configurations which are only accessible at high energy. This would include integrating over all field configurations involving A^μ, and those involving ψ with sufficiently large Euclidean four momentum. We can think of having some cut-off scale Λ where all field configurations with characteristic energy greater than Λ are “integrated out". The result can be re-expressed as a new path integral cut off at Λ with a new action and consequently a new Lagrangian density [16]. We call these quantities S_{eff} and $\mathscr{L}_{eff}$ respectively [17].

$$Z = \int^{\Lambda} \mathscr{D}\psi e^{iS_{eff}[\psi]} \tag{1.3}$$

$S_{eff}[\psi]$ will describe the physics of just ψ accurately at low energies [15] and when computing amplitudes it is significantly easier to use than employing $S[A,\psi]$ and taking the low energy limit at the end of the calculation. The obvious limitation with this method is that it is not immediately clear that performing the path integral is any less computationally intensive than working with the high energy theory. To avoid this task a formalism was developed to determine the most general form of the effective Lagrangian using the information from the high energy theory [18].

To construct a low energy theory one takes the set of fields which are still propagating degrees of freedom and writes down every possible interaction

that conforms to the symmetries of the high energy theory. This includes terms that will render the low energy theory non-renormalizable. The inclusion of these operators is the admission that this theory should eventually cease to be predictive at some energy scale where the dynamics of the vector boson become relevant. After doing this one matches the effective theory to the high energy theory at the scale Λ to determine the various coefficients of the low energy theory in terms of the parameters of the high energy theory. This is done by explicitly calculating various matrix elements and insisting the high and low energy theory yield the same result.

Since we are not truncating our operators in this effective Lagrangian density to preserve renormalizability we will in principle have to calculate an infinite number of diagrams to constrain all of the parameters of the theory. One might worry that this would rob the theory of all of its predictive power. In practice one is only interested in calculating a quantity to a fixed degree of accuracy; even with a renormalizable theory one typically must resort to a truncated perturbative expansion.

The action S must be dimensionless in natural units (i.e. it has the same units as $\hbar = 1$) we express this as $[S] = 0$. The action is defined by $S := \int \mathrm{d}^4x\mathscr{L}$ and so we have $[\mathrm{d}^4x] + [\mathscr{L}] = 0$ because in natural units length carries inverse dimensions we have $[\mathscr{L}] = 4$. This implies that in four dimensions if any operators appear in a theory that have dimensionality greater than four then they must be multiplied by some quantity which has

negative energy dimensions. This negative energy density turns out to be the cut off scale Λ [15] and as such we say processes are suppressed by that energy scale because all physical processes that involve that coupling will go like some polynomial in $\frac{E}{\Lambda}$ where E is the characteristic energy scale for that process.

We may take advantage of this suppression and truncate the effective Lagrangian by requiring a fixed degree of precision in our matching procedure, and since higher energy operators are suppressed by inverse powers of the cut off this truncation is justified. Thus if we only wish to calculate processes up to $\mathcal{O}\left(\frac{E^2}{\Lambda^2}\right)$ we would only include operators with energy dimension less than or equal to six. In the toy model of the weak interaction discussed above the lowest dimensional operator we can write down that is consistent with parity conservation after integrating out the vector boson is

$$\mathscr{L}_{eff} \supset G_F \overline{\psi}\psi\overline{\psi}\psi \tag{1.4}$$

($\overline{\psi}\gamma^5\psi\overline{\psi}\gamma^5\psi$ is equivalent by a Fierz identity) where G_F is a parameter of negative energy dimension whose relation to the high energy parameters will be derived below. So we must match the scattering amplitude for $\psi + \psi \rightarrow \psi + \psi$ in the high energy and low energy theories to ensure they have the same amplitude at the scale Λ. This corresponds to equating the matrix elements of the two Feynman diagrams shown in Figure 1.1. The propagator of the vector boson is given by

$$\langle 0|\, A^\mu(k)A^\nu(k)\,|0\rangle = -i\frac{g^{\mu\nu} - \frac{k^\mu k^\nu}{M^2}}{k^2 - M^2} \tag{1.5}$$

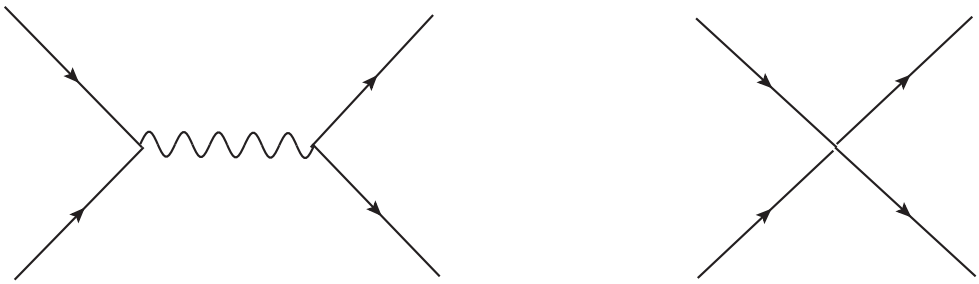

Figure 1.1: The diagram on the left shows $\psi + \psi \rightarrow \psi + \psi$ scattering in the high energy theory mediated by the massive vector boson. The diagram on the right is the same process in the low energy theory where the scattering is mediated by the dimension-six operator parameterized by G_F

[19] which goes as $\frac{-1}{M^2}$ in the low energy limit and so we see that

$$G_F \propto \frac{g^2}{M^2}\left[1 + \mathcal{O}\left(\frac{k^2}{M^2}\right)\right] = \frac{g^2}{M^2} \tag{1.6}$$

Where the final equality only holds in the low energy limit. The effects of the $\mathcal{O}\left(\frac{k^2}{M^2}\right)$ piece will be captured by higher-dimensional operators and as promised it is suppressed by appropriate powers of the relevant energy scale. This tells us that despite having an infinite number of operators in the Lagrangian our theory is predictive up to so fixed level of accuracy at a given energy scale. This is because higher-dimensional operators are suppressed at low energies.

The matching can also be obtained by setting the heavy field equal to its classical equation of motion with all momentum dependent terms set to

zero. In this case $\partial_\nu F^{\nu\mu} = M^2 A^\mu - g\bar{\psi}\gamma^\mu\psi$ so in momentum space

$$A^\nu = -\left(g^{\mu\nu} - k^\mu k^\nu - M^2\right)^{-1} g\overline{\psi}\gamma_\mu\psi = \frac{g}{M^2}\overline{\psi}\gamma^\nu\psi + \mathcal{O}\left(\frac{k^2}{M^2}\right) \tag{1.7}$$

substituting this into the original Lagrangian we can calculate G_F and we find

$$G_F\ \overline{\psi}\psi\overline{\psi}\psi := \frac{-g^2}{M^2}\overline{\psi}\gamma^\mu\psi\overline{\psi}\gamma_\mu\psi = 2\frac{g^2}{M^2}\ \overline{\psi}\psi\overline{\psi}\psi \tag{1.8}$$

and thus $G_F := 2\frac{g^2}{M^2}$. This procedure will only generate the some subset of the higher-dimensional operators however if that is all one needs it is a convenient method.

1.2 Accidental Symmetries of the Standard Model

Quantum field theories are often dictated by internal symmetries. The concept is essential for particle physics because one can show that a Lorentz invariant theory of massless spin one vector bosons implies an associated internal symmetry related to a Lie algebra [20]. Procedurally this means that to construct a quantum field theory with a set of massless spin one vector bosons, one specifies the gauge group of the theory G, the matter content, and the charge assignments and then writes down all possible combinations of fields which transform as a singlet under G. If one additionally insists that their theory be renormalizable the set of possible combinations must

be truncated so that no operators of energy dimension greater than four appear in the Lagrangian.

Dimension four is important because if a theory contains any operators of energy dimension greater than four their couplings must have negative energy dimension. The consequences of this are best understood with a specific example in mind. Let us consider our toy model from Equation 1.1. Here the parameter which controls the perturbative series is G_F which has energy dimension $[G_F] = -2$. This implies that the perturbation expansion will be controlled by the parameter $E^2 G_F$ and so at $E \approx G_F^{1/2}$ the perturbative expansion will break down [19]. This means that the theory is guaranteed to be invalidated at arbitrarily high energies and as such is non-renormalizable.

This truncation can result in the appearance of global symmetries which were not imposed on the model. This is because the combinations of operators which break these unintended global symmetries are all of dimension greater than four and as such have been excluded from the theory. These are known as accidental symmetries [13].

A toy model that illustrates this phenomena is scalar Q.E.D. with two scalars ϕ and ψ with charges Q and q respectively. The non-interacting part of the Lagrangian is qualitatively unaffected by charge assignments but the interactions we are allowed to write down are dictated by these

charge assignments. Let us examine two scenarios; one where $\frac{Q}{q} = -3$ and another where $\frac{Q}{q} = -4$. In these models the Lagrangian densities up to dimension-five operators are respectively

$$\mathscr{L} = \mathscr{L}_{QED} + V\left(|\phi|^2, |\psi|^2\right) + g\phi\psi^3 + h.c. \tag{1.9a}$$

$$\mathscr{L} = \mathscr{L}_{QED} + V\left(|\phi|^2, |\psi|^2\right) + \frac{g}{\Lambda}\phi\psi^4 + h.c. \tag{1.9b}$$

In both of these theories the potential is manifestly invariant under $\phi \to e^{i\theta}\phi$ and $\psi \to e^{i\omega}\psi$ where θ and ω are independent. These symmetries correspond to conservation of phions and psions respectively. The interaction terms in both theories break these symmetries by relating θ and ω, however had we demanded renormalizability the second Lagrangian would have been truncated prior to the appearance of the symmetry breaking operator and we would have an expanded set of global symmetries which were not imposed on the model. Note that the existence of these accidental symmetries is a non trivial result of the various fields' charge assignments.

It is worth discussing the phenomenological consequences of these accidental symmetries for each theory. For this discussion let us assume both scalars are massive and that $m_\phi >> 4m_\psi$. This means that the decay processes $\phi \to 3\psi$ and $\phi \to 4\psi$ are kinematically allowed. In the first theory, with the four point vertex, the former decay mode is allowed while in the the second theory, with the five point vertex, the latter is permitted. This is because the charge assignments of the two theories imply a conservation of $N_\phi - 3N_\psi$ and $N_\phi - 4N_\psi$ respectively where N_x is the x type particle number.

By dimensional analysis this means that any processes involving the dimension-five operator will be suppressed by factors of $g\frac{E}{\Lambda}$ as displayed in Figure 1.2 . So for energies much smaller than the cut off this operator is negligible. In the context of our theory this implies that phions will be meta-stable at low energies provided $m_\phi << \Lambda$ since the relevant energy scale for the decay process is the mass of the phion. We can see that charge assignments can dictate much more than just the strength of a particles interaction with the gauge group.

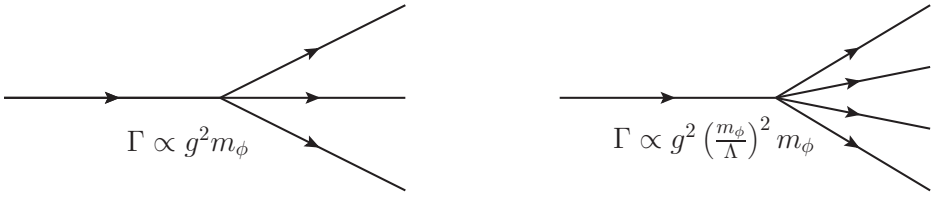

Figure 1.2: Leading order $\phi \to 3\psi$ decay process for the two charge assignment choices with the right diagram corresponding to 1.5(b) and the left diagram corresponding to 1.5(a)

The Standard Model contains four accidental $U(1)$ symmetries corresponding to the conservation of B, L_e, L_μ, and L_τ [20] (baryon number, and each generation's lepton number). The latter three of the listed symmetries are only exactly realized in a model with massless neutrinos. These symmetries are incompatible with data from neutrino oscillation experiments [3]. The breaking of these three symmetries is the result of the inclusion of an extra dimension-five operator [21] and this suggests the Standard Model is just

some effective low energy limit of another theory, which in turn points to the existence of some high energy physics which is not encoded in the Standard Model. The observations of neutrino oscillations still permit two accidental symmetries B and $L := L_e + L_\mu + L_\tau$[20].

1.3 Anomalous Symmetries

In classical physics, symmetries of the action manifest themselves as conserved quantities [22]; in field theory these are conserved currents. One might expect that this statement holds true in quantum physics as well. This is often the case, however sometimes quantum corrections break the symmetry; these are known as anomalous symmetries [23, 24]. This occurs when the classical action is invariant under a symmetry transformation but the functional measure is not. In the path integral formalism, the partition function Z fully defines a theory and is given by

$$Z = \left[\prod_{i=0}^{n} \int \mathscr{D}\phi_i \right] \; e^{S_{cl}[\phi_1, \phi_2, \ldots, \phi_n]} \tag{1.10}$$

We see that the requirement that the classical action be invariant under a symmetry transformation is not sufficient; we also need the functional measure to remain invariant. We can quantify this anomalous behaviour for a symmetry which is realized by a set of fields transforming in an irreducible representation R of a symmetry group S by its anomaly coefficient $A_R(S)d^{abc} := \frac{1}{2} Tr\left(\{T_R^a, T_R^b\} T_R^c\right)$ where $\{T_R^a\}$ are the set of generators for the symmetry group S in the representation R. For reducible representations

$R = R_1 \oplus R_2$ we have $A_R(S) = A_{R_1}(S) + A_{R_2}(S)$. For a non-anomalous symmetry $A_R(S) = 0$ for all representations of that symmetry group present in the theory[25].

To determine these anomaly coefficients one can calculate $\langle p,k|\partial_\mu J^\mu|\Omega\rangle$ where J^μ is the Noether current associated with the symmetry, $|\Omega\rangle$ is the vacuum, and $\langle p,k|$ corresponds to two gauge boson final states. In a theory with no gauge bosons it is consistent for a symmetry to become anomalous however if the Noether current J^μ couples to a gauge field A_μ then for the ward identities to be preserved the anomaly must vanish. In the case of this coupling the anomaly coefficient $A_R(S)$ can be can be computed via the triangle diagrams shown in Figure 1.3 [26]. The trace over generators and anti-commutator in the definition of the anomaly coefficient can be understood by the loop structure of the fermions and the Bose statistics of the two outgoing states respectively. Thus $A_R(S)$ is a measure of the degree to which quantum corrections break a classical symmetry. For the accidental symmetries of the Standard Model $A(B) = 1$ while for the lepton numbers $A(L_i) = 1$ where $i \in \{e,\mu,\tau\}$[20]. As a result, any linear combination of these symmetries whose anomaly coefficients cancel is an exact symmetry of the quantum theory. The more popularly considered options in the literature are $B-L$ and $L_i - L_j$ where $i,j \in \{e,\mu,\tau\}$ and to avoid triviality $i \neq j$ [27].

Of all the possible symmetries of the form $L_i - L_j$ the one which is least

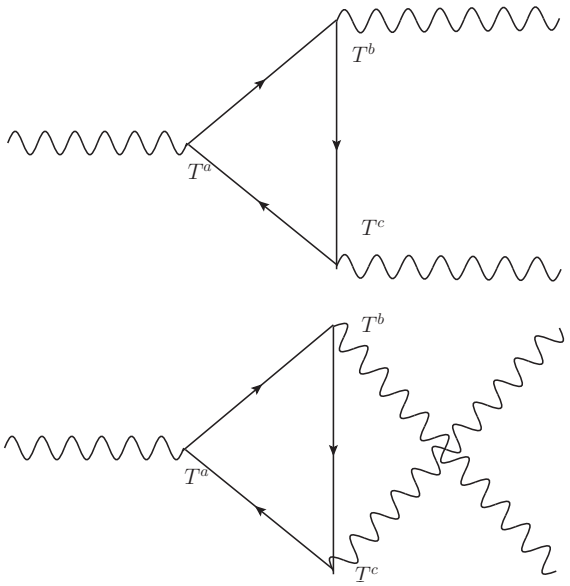

Figure 1.3: Triangle diagrams used to calculate anomaly coefficient for gauge symmetries

tightly constrained by experiment is $L_\mu - L_\tau$. This is due to the relative abundance of high precision experiments involving electrons compared to those involving muons or tauons. Experiments involving the higher mass leptons are difficult to conduct due to the instability of muons and tauons.

One important consequence of a symmetry being anomalous is that it cannot couple to a gauge field in one's theory. This is because without the conservation of a charge the Ward identities are destroyed and the theory becomes gauge dependent.

1.4 Neutrino Oscillations

Quark masses are generated in the Standard Model by operators of the form

$$\mathscr{L}_{SM} \supset f_{ij} Q_i H d_j^c + g_{ij} Q_i \tilde{H} u_j^c \tag{1.11}$$

[13] where $Q_i := (u_i, d_i)^T$ is the left handed $SU(2)$ doublet of two component left handed spinor quark fields, u_j^c and d_j^c are left handed two component spinors that are a singlet under $SU(2)$ and i and j index the various generations of the quarks. H is the Higgs doublet and $\tilde{H} := -i\sigma_2 H^*$. After electroweak symmetry breaking these operators give mass terms which can be seen by replacing the Higgs field H by its vacuum expectation value $(0, \langle h \rangle)^T$

$$\mathscr{L}_{SM} \supset \langle h \rangle f_{ij} u_i u_j^c + \langle h \rangle g_{ij} d_i d_j^c \tag{1.12}$$

These terms can be diagonalized by writing each set of fields in a new basis $u_i' = P_{ij} u_j$ and $d_i' = R_{ij} d_j$. The existence of the right handed quark fields u_i^c and d_j^c are what allow for both up and down type quarks to have masses.

In the broken phase, charged current interactions in the Standard Model are of the form $g_2 \overline{d}_i \sigma^\mu W_\mu^- u_i$ and as a result when written in the mass basis these interactions take the form $g_2 V_{ij} \overline{d}_i' \sigma^\mu W_\mu^- u_j'$ where $V_{ij} := R_{ik}^\dagger P_{kj}$ is known as the Cabibbo-Kobayashi-Maskawa (CKM) matrix [28, 29]. The basis in which the mass matrix for the quarks is diagonal define the basis whose fields' excitations can be interpreted as asymptotic states. By requir-

ing that we write our interactions in this basis we have fixed R and P and thus V_{ij} cannot in general be chosen to be diagonal.

In the lepton sector the story is identical except that there is no analogue for u_i^c. We have a set of right handed charged leptons e_i^c but no right handed neutrinos. This absence of mass terms for the neutrinos leaves R to be freely chosen to diagonalize the charged current interactions. This means that in the Standard Model all leptons couple diagonally in the mass basis. Resultantly there are no terms that couple different generations of leptons to one another so each generation can transform independently under its own $U(1)$ symmetry. This is why there are three lepton symmetries and only one Baryon symmetry. The lepton generational symmetries also forbid processes like $\nu_e \to \nu_\mu$ because this would violate two of the conserved charges (L_e and L_μ); this is an example of a neutrino oscillation.

Neutrino oscillations have been observed [2, 3] and because oscillations are forbidden by the symmetries listed above we know that the Standard Model is incomplete. Without adding additional matter content to the model to explain the observed non-conservation of generational lepton number one is forced to abandon renomalizability and include the dimension-five operator [21]

$$\mathscr{L} \supset \frac{y_{ij}}{\Lambda}\left(L_i\tilde{H}\right)\left(L_j\tilde{H}\right) \to y_{ij}\frac{\langle h\rangle^2}{\Lambda}\nu_i\nu_j \tag{1.13}$$

This is known as the Weinberg operator [21] and after symmetry breaking

it results in a mass matrix of the same form as in the quark sector. This breaks L_e, L_μ and L_τ because the freedom to use R to diagonalize the interactions with the gauge bosons is saturated due to the requirement that the neutrino mass matrix be diagonal. Thus any theory which expands the matter content of the Standard Model to explain neutrino oscillations with Majorana neutrinos should generate this operator in its effective low energy description provided the Majorana mass scale is significantly larger than the Dirac mass scale. There does exist the possibility of a vanishing Majorana mass scale which would make the neutrino a Dirac type particle. Neutrinoless double beta decay searches are actively investigating this possibility [30].

1.4.1 PMNS Matrix

The analogue of the CKM matrix is known as the Pontecorvo-Maki-Nakagawa-Sakata (PMNS) matrix [31]. It is no longer trivially diagonal due to the presence of a left handed neutrino mass matrix. It's standard parametrization is given by

$$\begin{bmatrix} \nu_e \\ \nu_\mu \\ \nu_\tau \end{bmatrix} = \begin{bmatrix} c_{13}c_{12} & -c_{13}s_{12} & s_{13}e^{-i\delta} \\ -s_{23}s_{13}c_{12}e^{i\delta} - c_{23}s_{12} & -s_{23}s_{13}s_{12}e^{i\delta} + c_{23}c_{12} & s_{23}c_{13} \\ -c_{23}s_{13}c_{12}e^{i\delta} + s_{23}s_{12} & -c_{23}s_{13}s_{12}e^{i\delta} - s_{23}c_{12} & c_{23}c_{13} \end{bmatrix} \begin{bmatrix} \nu_1 \\ \nu_2 \\ \nu_3 \end{bmatrix} \quad (1.14)$$

where the left hand side are the flavour basis states, the right hand side are the mass eigenstates and $s_{ij} = \sin\theta_{ij}$ and $c_{ij} = \cos\theta_{ij}$. The angles θ_{12}, θ_{13} and θ_{23} parametrize the mixing between ν_1 and ν_μ, ν_1 and ν_τ, and ν_2

and ν_τ respectively. The parameter δ measures the amount of CP violation and is zero for real Yukawa couplings and the mixing angles measure the relative abundance of electron, muon and tauon type neutrinos in each mass eigenstate.

1.4.2 Mixing Data

An important aspect of neutrino data is that there are two discreetly separated regions of parameter space [32]. This is because the sign Δm^2_{13} is still undetermined. As a result it is not clear whether the neutrino mass spectrum is such that ν_1 is the lightest eigenstate or ν_3; in contrast it is known that $m_2 > m_1$. These two possibilities are referred to as the normal and inverted hierarchies respectively and are denoted NH and IH.

The listed data in Table 1.1 [8] is from the most recent release of nu-fit at the time of this writing. $\Delta m^2_{ij} := m^2_i - m^2_j$ where m_i is the i^{th} eigenvalue of the left handed mass matrix. The precision in measuring δ is extremely poor and as a result for this research we assume real Yukawa couplings and no CP violation for this work. In this paper we will be fitting from data from nuFit which provides a global fit to neutrino data. The data does not correspond to any single experiment.

NuFIT 2.0 (2014)

	Normal Ordering ($\Delta\chi^2 = 0.97$)		Inverted Ordering (best fit)		Any Ordering
	bfp $\pm 1\sigma$	3σ range	bfp $\pm 1\sigma$	3σ range	3σ range
$\sin^2\theta_{12}$	$0.304^{+0.013}_{-0.012}$	$0.270 \to 0.344$	$0.304^{+0.013}_{-0.012}$	$0.270 \to 0.344$	$0.270 \to 0.344$
$\theta_{12}/^\circ$	$33.48^{+0.78}_{-0.75}$	$31.29 \to 35.91$	$33.48^{+0.78}_{-0.75}$	$31.29 \to 35.91$	$31.29 \to 35.91$
$\sin^2\theta_{23}$	$0.452^{+0.052}_{-0.028}$	$0.382 \to 0.643$	$0.579^{+0.025}_{-0.037}$	$0.389 \to 0.644$	$0.385 \to 0.644$
$\theta_{23}/^\circ$	$42.3^{+3.0}_{-1.6}$	$38.2 \to 53.3$	$49.5^{+1.5}_{-2.2}$	$38.6 \to 53.3$	$38.3 \to 53.3$
$\sin^2\theta_{13}$	$0.0218^{+0.0010}_{-0.0010}$	$0.0186 \to 0.0250$	$0.0219^{+0.0011}_{-0.0010}$	$0.0188 \to 0.0251$	$0.0188 \to 0.0251$
$\theta_{13}/^\circ$	$8.50^{+0.20}_{-0.21}$	$7.85 \to 9.10$	$8.51^{+0.20}_{-0.21}$	$7.87 \to 9.11$	$7.87 \to 9.11$
$\delta_{\rm CP}/^\circ$	306^{+39}_{-70}	$0 \to 360$	254^{+63}_{-62}	$0 \to 360$	$0 \to 360$
$\frac{\Delta m^2_{21}}{10^{-5}\ \text{eV}^2}$	$7.50^{+0.19}_{-0.17}$	$7.02 \to 8.09$	$7.50^{+0.19}_{-0.17}$	$7.02 \to 8.09$	$7.02 \to 8.09$
$\frac{\Delta m^2_{3\ell}}{10^{-3}\ \text{eV}^2}$	$+2.457^{+0.047}_{-0.047}$	$+2.317 \to +2.607$	$-2.449^{+0.048}_{-0.047}$	$-2.590 \to -2.307$	$\begin{bmatrix} +2.325 \to +2.599 \\ -2.590 \to -2.307 \end{bmatrix}$

Table 1.1: Data from nu-Fit after fitting to global data from 'NOW' conference in 2014 [8]. This table is taken from the nu-Fit collaboration website (2015)

1.4.3 See-Saw Mechanism

Suppose we include a new set of three fields which are singlets under the Standard Model gauge group denoted N_i where $i \in \{e, \mu, \tau\}$

$$\mathscr{L} \supset \bar{N}_i(-i\partial\!\!\!/)N_i - \frac{1}{2}M_{ij}N_iN_j + y_{ij}N_i\left(L_j\tilde{H}\right) + h.c. \tag{1.15}$$

and we take all of the eigenvalues of the Majorana mass matrix to be much larger than the relevant energy scale. Then we can integrate out the fields N_i by setting them equal to their classical equation of motion in the limit of low momenta.

$$M_{ij}N_j = -i\partial\!\!\!/N_i - y_{ik}\left(L_k\tilde{H}\right) \to N_j = M^{-1}_{ji}y_{ik}\left(L_k\tilde{H}\right) \tag{1.16}$$

where the derivative has been dropped due to its momentum dependence (see Equation 1.1). Substituting Equation 1.4.3 back into the Lagrangian in Equation 1.4.3 and performing a phase shift on the leptonic fields $L_i \rightarrow \exp i\pi/2\, L_i$ we obtain

$$\mathscr{L}_{IR} \supset -\frac{1}{2}\left(Y^T M^{-1} Y\right)_{ij} \left(L_i \tilde{H}\right)\left(L_k \tilde{H}\right) \tag{1.17}$$

this is exactly the Weinberg operator from Equation 1.4. The left handed neutrino mass matrix can be identified as

$$M^{(L)} = \langle h \rangle^2 Y^T M^{-1} Y \tag{1.18}$$

where $\langle h \rangle$ is the Higgs vacuum expectation value. Excluding neutrinos, known lepton masses lie within the range of $0.5 - 2000$ MeV. In the Standard Model all of these masses are generated via the Higgs mechanism and as a result this is a statement about the relative magnitudes of their Yukawa couplings lying within a range spanning about four orders of magnitude. In contrast the heaviest neutrino mass is constrained to be less than about 0.1 eV [14] which is six orders of magnitude lower than the mass of the electron. If we naively expect that this mass is also generated via electroweak symmetry breaking then this is a startling statement about he size of the neutrinos' Yukawa couplings relative to those of the other leptons.

In contrast to other leptons a right handed neutrino's mass need not be generated via the Higgs mechanism and as a result a disparity in its mass

compared to Standard Model leptons would not be surprising. Parametrically the see-saw mechanism gives

$$m_\nu \approx y \langle h \rangle \frac{y \langle h \rangle}{M_N} \tag{1.19}$$

where m_ν is the mass of the neutrino M_N is the Majorana mass of the sterile neutrino and $y \langle h \rangle$ is the Dirac mass. So provided the mass scale of the right handed neutrinos is sufficiently large compared to its Higgs generated Dirac mass (which may be of the same order as the other leptons) this mechanism can give a natural explanation of the small neutrino masses without disparate ratios between the various Yukawa couplings.

1.5 Dark Matter

Astronomers have noted peculiar rotation curves for various galactic systems since as early as 1933 [33–38]. These systems are peculiar because if one assumes that luminous mass is the sole cause of gravitation in the system the velocity of various orbiting bodies violate the virial theorem [34–38].

One solution to this problem is to postulate the existence of some form of matter whose coupling to electromagnetism is sufficiently weak such that it cannot be observed directly. This matter would still have an energy density and as a result couple to gravity; this is dark matter. Its existence allows for rectification of the rotation curves mentioned above with our current

understanding of gravity by providing the additional gravitational potential energy necessary for the virial theorem to hold.

Evidence for the existence of dark matter also comes from gravitational lensing data [39]. One system, known as the bullet cluster, is particularly important in the experimental justification of dark matter. The system consists of two separate galactic dust clouds which collided in the past. Gravitational lensing has shown that the mass distribution of the cluster is partially luminous and partially non-luminous. The non-luminous mass's distribution is not indicative of a collision while the luminous bayonic mass has been slowed significantly [40]. This is suggestive of dark matter's self interaction being significantly weaker than those of Standard Model particles and results in a bound on the self interaction cross section of dark matter [41].

Along with astrophysical data, dark matter's interaction with Standard Model particles must be considered. Two distinct sub-classes of interactions can constrain dark matter in different ways. The first of these is known as direct detection. This method involves low background experiments that search for kinetic transfer between a dark matter particle and some observable standard model particle; most often an atomic nucleus. These experiments can then place bounds on the coupling of the dark matter particle relative to it's mass [42–46]; for a review see [47].

The second way to probe dark matter's interactions with Standard Model particle content is to look for dark matter annihilation signatures of the form $\chi + \bar{\chi} \rightarrow SM$ as well as decay signatures like $\chi \rightarrow SM$ where χ is used to denote the dark matter candidate; this is known as indirect detection [48, 49]. The Standard Model products are observable and so searches can be conducted to place bounds on parameters in particular dark matter theories. These process $\chi \rightarrow \gamma + \nu$ will be discussed in greater detail in the context of sterile neutrino dark matter.

Finally theories that propose dark matter candidates must examine if their model agrees with cosmological predictions from the early universe. Adding new species can create observable changes in the cosmic microwave background, lead to overpopulation of various standard model species via decays and result in relic abundances of dark matter that do not agree with observations. The latter forces one to consider production mechanisms that would create the correct amount of dark matter in the universe today, these can be partitioned into two categories; thermal and non-thermal production.

Thermal production assumes that at some early epoch of the universe the dark matter comes into thermal equilibrium with the photon bath via some interaction that leads to a temperature dependent cross section. At some later epoch the thermalizing cross section becomes sufficiently small due to the lower temperature and the mean free path of dark matter particle exceeds the Hubble length. This means that the universe is expanding

faster than the dark matter candidate can react with the Standard Model bath resulting in it's departure from thermal equilibrium [50]. As a result the dark matter "freezes out" and maintains its temperature at freeze-out (see Figure 1.5). This scenario is insensitive to the initial conditions of the universe and is almost exclusively determined by the dark matter's interaction cross section with the Standard Model; the greater the cross section the lower the relic abundance.

Non-Thermal production, in contrast, is sensitive to the initial conditions of the universe. The mechanism relies on the production of dark matter in a latter epoch of the universe. This dark matter never comes into thermal equilibrium due to its feeble interactions with the primordial soup of particles and after the production mechanism terminates the dark matter is sufficiently stable to leave a relic abundance of dark matter particles. A concrete example of this mechanism is the decay of a massive particle into dark matter. Once the temperature drops below approximately half the mass of the progenitor decay is possible but production becomes kinematically disallowed. The progenitor species will be depleted by decay and the remaining dark matter candidates will not be able to thermalize due to its weak interaction cross section with the remaining soup of particles [51].

There are three major classifications of dark matter: hot $\left(T_\chi >> M_\chi\right)$, cold $\left(T_\chi << M_\chi\right)$ and warm $\left(T_\chi \approx M_\chi\right)$ where T_χ is the temperature of the dark matter when galaxy sized masses enter the horizon [52]. Hot dark matter

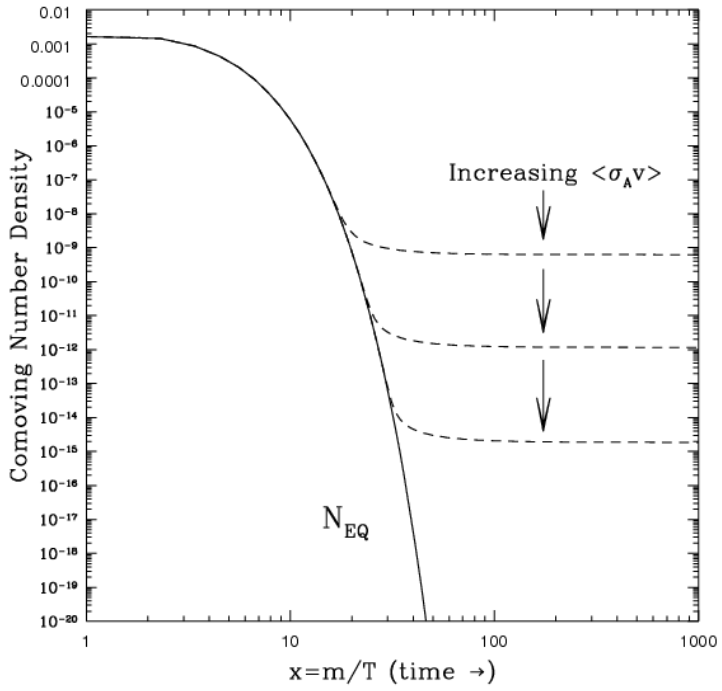

Figure 1.4: A schematic diagram showing a freeze-out scenario. The dark matter species remains in equilibrium until some critical temperature and then it decouples from the photon bath resulting in a relic abundance. Figure taken from Hooper (2009) [10]

fails to form galaxies a due to its high velocity and its correspondingly long free streaming length [6]. If one assumes dark matter is mostly hot one makes predictions that disagree with observations and as a result hot dark matter cannot account for all of the observed energy density. This is what rules out active neutrinos as a dark matter candidate their free streaming length is so long that they wash out the formation of structure in the galaxy.

Models of structure formation have previously favoured warm dark matter however more recent simulations that incorporate baryonic effects found that both cold and warm dark matter remain viable possibilities [53]. For sterile neutrinos the possibility of hot dark matter is still viable due to its unconstrained mass scale. The lower bound for structure formation mass is given by $M_{SF} \approx 3 \cdot 10^{15} \left(\frac{30\text{eV}}{m_\nu}\right)^2 \Omega_\nu^{-1} M_\odot$ [54] where Ω_ν is the energy density fraction of neutrino dark matter, $M_\odot$ is the mass of the sum and m_ν is the mass of the sterile neutrino dark matter candidate. and as such for higher masses the minimum mass required for structure formation can be lowered to the necessary $10^6 M_\odot$ [52] by considering sterile neutrinos with sufficiently large m_ν.

1.6 Sterile Neutrinos as Dark Matter

A natural candidate one may consider for dark matter are the Standard Model neutrinos. They are known to be massive, interact via only the weak interaction and most importantly their existence is experimentally verified, however bounds on large structure formation prohibit the Standard Model neutrino from being a viable candidate to account for all of the observed dark matter [6]. Standard Model neutrinos must be relativistic because $T_\nu \approx 2\text{eV}$ while measurements of the cosmic microwave background force $m_\nu \lesssim 0.1\text{eV}$ [55]. As such neutrinos destroy large scale structure by the argument given in the previous section due to their ultra light mass.

Right handed neutrinos can be expected to exist for the reasons given above and they are a suitable dark matter candidate. Since their mass scale is not fixed, whether or not they classify as warm or cold dark matter is dictated by parametrics. The production method for sterile neutrino dark matter that is of interest for this paper has its roots in the 1993 proposal by Dodelson and Widrow [54]. The concept was to rely on non-thermal production of dark matter via neutrino oscillations. Oscillations are dictated by the relative right and left handed neutrino content of propagating mass eigenstates. During interactions with Standard Model particles a mostly sterile mass eigenstate can be generated if it has a small active component.

This is related to the diagonalization of the mass matrix which contains both Majorana and Dirac masses; because the mass matrix is symmetric the relative quantity of right and left handed neutrinos can be parametrized by a mixing angle θ_m. In the see-saw limit at zero temperature this angle is given by $\theta_0 = \frac{y\langle h \rangle}{M}$ however at higher temperatures this angle is corrected. Since the early universe is a hot and dense primordial soup of particles these high temperature effects are important. The temperature dependent mixing angle takes the form

$$\sin^2 2\theta_m = \frac{\sin^2 2\theta_0}{\sin^2 2\theta_0 + [\cos 2\theta_0 + \Delta_R(k,T)]^2} \tag{1.20}$$

Where $\Delta_R(k,T)$ is related to the contribution to the neutrino self energy from vector-boson exchange [56, 57] and is composed of corrections from Standard Model processes and a Z' correction [7]. At zero temperature

the corrections vanish, however at high temperatures the mixing angle is suppressed. The high temperature behaviour of the Standard Model contribution to $\Delta_R(k,T)$ is given by

$$\Delta_R^{(SM)}(k,T) = \frac{28\pi \sin^2\theta_W G_F T^4 k^2}{45\alpha m_s} \tag{1.21}$$

[56, 57] where G_F is the Fermi constant, θ_W is the Weinberg angle, m_s is the mass of the sterile neutrino dark matter candidate, and α is the fine structure constant. Therefore in early epochs of the universe, neutrino production would not result in transformations into the sterile state due to the strong mixing angle suppression from high temperature effects.

Then in some intermediate epoch the active to sterile transformations would become significant enough to produce sterile neutrinos but not sufficient to allow them to reach equilibrium. Finally, at the time of neutrino freeze-out, neutrinos decouple from the bath and cease to have interactions that would allow for transformation into sterile states. Thus the population of sterile states becomes decoupled and represents a possible dark matter candidate.

Bounds on models of sterile neutrinos come from many sources: neutrinoless double beta decay, big bang nucleosynthesis, cosmic microwave background measurements, x-ray telescopes and large scale structure formation [58]. For this thesis the bounds from x-ray emission are our primary concern. If dark matter is composed of sterile neutrinos there are two bounds one must satisfy. These are related to the possibility of decays such as $N_1 \to \nu + \gamma$

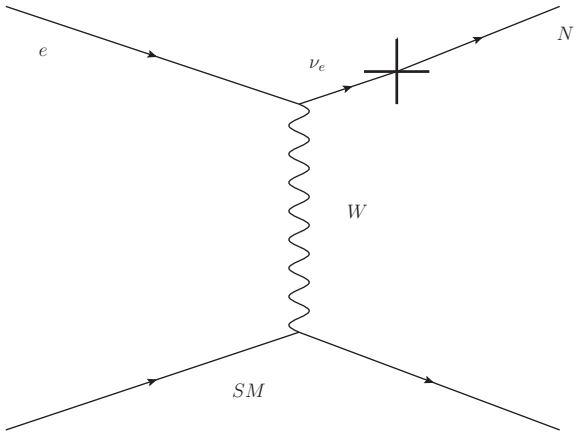

Figure 1.5: An example of a process that contributes to the production of a sterile neutrino abundance via transformation of an electron into an electron neutrino (written in flavour basis) which composes some small component of the mass eigenstate N. As a result there is a non-vanishing probability of "transforming" an electron into a sterile neutrino.

which are mediated at the one loop level by process shown in Figure 1.6. The decay rate for these processes is given by [58]

$$\Gamma = \frac{1}{1.8 \cdot 10^{21}\mathrm{s}} \sin^2\theta_m \left(\frac{m_s}{\mathrm{keV}}\right)^5 \tag{1.22}$$

The first concern is to ensure that the decay rates from these diagrams are sufficiently small to ensure a cosmologically stable lifetime. Even for decay rates which are sufficiently small to ensure that the dark matter is stable, decay signals involving photons can still be detectable [48]. This is because of the large number density of sterile neutrinos that would be required to explain the observed dark matter abundance. Even if the decay

rate of a single dark matter particle is negligible, if it is non vanishing it will eventually yield an observable signal for a sufficiently large number density.

The large number density of sterile neutrinos to yield the correct dark matter energy density means that decays such as those shown in Figure 1.6 can be relevant even for very small decay rates. We are interested in the quantity $n_\chi \Gamma_\chi$ where n_χ is the number density of the dark matter. The energy density of the dark matter, if it is entirely composed of non-relativistic sterile neutrinos, is given by $n_\chi m_s$ and as a result for a given m_s the number density is fixed. Equation 1.6 depends on only two free parameters m_s and $\sin^2\theta_m$ however because the production of the dark matter is mediated by known (Standard Model) physics. In the Dodelson Widrow scenario for a given m_s the only free parameter left to determine the relic abundance of sterile states is θ_m. As such in a plot of $\sin^2\theta_m$ vs m_s there is only a narrow band in which the Dodelson Widrow scenario is valid.

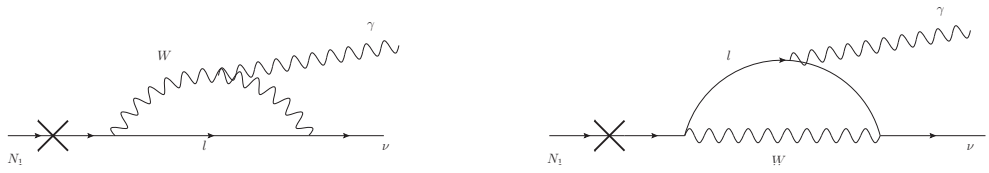

Figure 1.6: Primary decay mode for a heavy sterile neutrino $N \to \nu + \gamma$ via a loop process with a charged W boson and any Standard Model fermion charged under $SU_W(2)$ resulting in the emission of a neutrino and a photon.

By searching for x-ray signals in regions of the sky with known dark matter densities this two dimensional parameter space can be probed to test the validity of the Dodelson Widrow dark matter scenario. Galactic x-ray searches have failed to discover such a signal and this lack of observation establishes bounds constraining the mixing angle of sterile neutrinos for various possible masses. Boyarsky *et. al.* [11] looked for these x-rays in the Milky Way galaxy where there is a known density of dark matter. Their results are shown in Figure 1.7. The lack of observation of galactic x-rays has ruled out the Dodelson Widrow scenario if it is mediated by Standard Model interactions and has pushed the bounds on $\sin^2 2\theta_m$ all the way down to 10^{-10} for $m_s \approx 10$ keV.

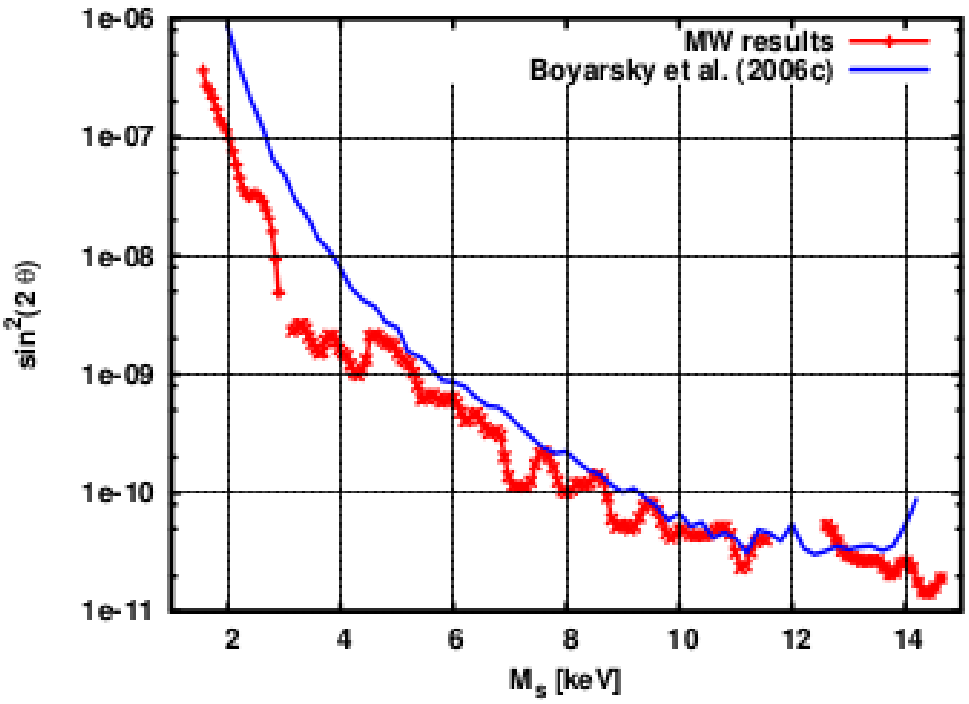

Figure 1.7: Constraints on sterile neutrino dark matter from observations of the Milky Way [11]. Figure taken from Boyarsky *et. al.* (2006).

CHAPTER 2

OVERVIEW OF THE PROPOSED MODEL

Our model supposes the existence of three right-handed neutrinos and an additional vector boson that couples to the charge $L_\mu - L_\tau$. The inclusion of this additional vector boson necessitates a mass generating mechanism [7]. One possibility is an order parameter which spontaneously breaks the $U'(1)$ symmetry this is known as the Higgs mechanism [26, 59]. This can be achieved via a complex scalar field that couples to the Z' and thus must be charged under the new gauge group. Its charge relative to the sterile neutrinos is fixed by phenomenological requirements. Our choice of charge assignments are presented in Table 2.1.

Field	$U_Y(1)$	$SU(2)$	$U_{L_\mu - L_\tau}(1)$
N_e	0	$\mathbb{1}$	0
N_μ	0	$\mathbb{1}$	-1
N_τ	0	$\mathbb{1}$	1
L_μ	$-\frac{1}{2}$	2	1
L_τ	$-\frac{1}{2}$	2	-1
L_e	$-\frac{1}{2}$	2	0
H	$-\frac{1}{2}$	2	0
S	0	$\mathbb{1}$	1

Table 2.1: Charge assignments of the relevant fields under hypercharge $SU_W(2)$and the new $U'(1)$. Here 2 refers to the fundamental representation of $SU(2)$.

The order parameter responsible for the generation of a massive Z' is denoted by S. N_i are left-handed two component spinors that are singlets under the Standard Model gauge group and the rest of the fields are the familiar Standard Model matter content (see Appendix A). Writing down the most general renormalizable Lagrangian density consistent with the matter content and charge assignments, one arrives at

$$\mathscr{L} = \mathscr{L}_{SM} + \mathscr{L}'_{kin} + \mathscr{L}'_{Yuk} - V\left(S^\dagger S\right) \tag{2.1a}$$

$$\mathscr{L}'_{kin} = \overline{N}_i \overline{\not{D}} N_i - \frac{1}{4} F'^{\mu\nu} F'_{\mu\nu} + \left(D_\mu S\right)^\dagger \left(D^\mu S\right) + h.c. \tag{2.1b}$$

$$\mathscr{L}'_{Yuk} = y_i \left(L_i \tilde{H}\right) N_i + \frac{1}{2} M_e N_e N_e + M N_\mu N_\tau + g_\mu N_\mu N_e S + g_\tau N_\tau N_e S^\dagger + h.c. \tag{2.1c}$$

$$V\left(S^\dagger S\right) = \frac{\lambda_S}{2}\left(S^\dagger S - \frac{\langle S\rangle^2}{2}\right)^2 \tag{2.1d}$$

D_μ is the covariant derivative for each field whose charges are dictated by Table 2.1. The notation of slashes with (without) an overbar correspond to contraction with $\overline{\sigma}^\mu$ (σ^μ) and all spinors are two component Weyl spinors. Kinetic mixing terms between the photon and the Z' such as $F_{\mu\nu}F'^{\mu\nu}$ are forbidden by upper bounds on the photon's mass. Here we have elected to include the mass matrix with the Yukawa terms for future convenience. The gauge coupling constant is the only parameter not explicitly appearing in the Lagrangian density and will be denoted g'. Additionally we must augment the Standard Model covariant derivatives for μ and τ generation leptons to include their coupling to the new Z'.

2.1 Phases of Parameters

It is worth developing a convention for the phases of various parameters so that consistency is maintained when comparing bounds from different sources. Despite being interested in a CP conserving limit for our analysis fixing the phase of a parameter can guarantee its positivity. This may in turn render certain solutions obsolete if they require said parameter to be negative.

By re-phasing fields in our theory we can demand that a fixed number of parameters are real and positive, however the number of independent re-phasings we can perform is limited by the number of fields at our disposal. As a result only some subset of our parameters will have their phase fixed with the remaining parameters free to take on any complex value. We will be interested in a CP conserving limit and so the phase freedom of the unfixed parameters allows for the possibility of them taking on negative values.

Let us begin with the singlet scalar field. Here we define the phase of the field to be such that when the symmetry is spontaneously broken the breaking pattern is such that the field's vacuum expectation value is entirely real. This fixes the phase of the complex field S.

Next we examine the right-handed neutrinos. Let us first re-phase N_e to force M_e to be positive this will modify the phase of both g_μ and g_τ however we may then fix the phase of both of these parameters by using the freedom provided by the fields N_μ and N_τ. This leaves the phase of M undetermined since it is the result of coupling between N_μ and N_τ and these fields' phases have been fixed.

For the Yukawa couplings we are free to re-phase the Standard Model leptonic fields L_i and so we can fix the phase of all of our Yukawa couplings but after doing so we have exhausted all of our degrees of freedom. Thus of

the parameters controlling neutrino mixing only M may take on negative values.

The fact that only one parameter that is related to neutrino mixing in our theory is not fixed to be positive is a result of the Yukawa couplings being diagonal and the lower 2x2 block of the mass matrix having only one independent entry. Had there been additional operators in our theory which induced couplings in the lower 2x2 block their phases would not be fixed. This is important because we will be considering modifications to the presented theory which involve dimension-five operators in the listed entries. As a result their phases will not be fixed and they can take on negative values.

2.2 Consequences of Singlet Symmetry Breaking

2.2.1 A Massive Z'

The spontaneous breaking of the $U'(1)$ symmetry was motivated by the generation of a mass for the new Z' gauge boson. It is worth examining this mechanism in detail and reviewing Faedev-Poppov gauge fixing procedure in the context of our model [26]. In the context of the Higgs mechanism we wish to excite our fields about the minimum energy state or true vacuum

[26]. In the case of the potential in our theory there are infinitely many degenerate vacuua that minimize the potential.

$$V\left(|S|^2\right) = \frac{\lambda}{4}\left(|S|^2 - \frac{\langle S\rangle^2}{2}\right)^2 \tag{2.2}$$

The vacuum solution is manifest and is given by $S = \frac{1}{\sqrt{2}}\langle S\rangle e^{i\theta}$. We may choose to expand our field about the vacuum with $\theta = 0$ with no loss of generality. We are therefore interested in the quantum excitations about this field configuration and so we should choose to write

$$S = \frac{1}{\sqrt{2}}(\langle S\rangle + \sigma)e^{i\pi/\langle S\rangle} \tag{2.3}$$

and interpret the quanta of σ and π as particle states. Here π is the Nambu-Goldstone boson and σ is the remaining gapped degree of freedom. Gapped refers to the finite amount of energy required to excite a one particle state. The field π is normalized by $\langle S\rangle$ so that it will be canonically normalized. Writing the field this way emphasizes that the $U'(1)$ symmetry is realized non-linearly. If we substitute this into the kinetic term for the singlet field we obtain

$$\begin{aligned}\mathscr{L} \supset & \left[\left(\partial_\mu + ig'Z'_\mu\right)\frac{1}{\sqrt{2}}(\langle S\rangle + \sigma)e^{-i\pi/\langle S\rangle}\right]\left[\left(\partial^\mu - ig'Z'^\mu\right)\frac{1}{\sqrt{2}}(\langle S\rangle + \sigma)e^{i\pi/\langle S\rangle}\right] \\ & = \frac{1}{2}(\partial\sigma)^2 + \frac{1}{2}g'^2\left(Z'_\mu - \frac{1}{g'}\partial_\mu\frac{\pi}{\langle S\rangle}\right)\left(Z'^\mu - \frac{1}{g'}\partial^\mu\frac{\pi}{\langle S\rangle}\right)(\langle S\rangle + \sigma)^2\end{aligned} \tag{2.4}$$

If we take the limit where $g' = 0$ we see that the kinetic term for the Goldstone mode is canonically normalized as promised. If we now expand the final term and recognize that the new field strength tensor $F'^{\mu\nu}$ is

invariant under gauge transformations we can take $Z'_\mu \to Z'_\mu + 1/g'\partial_\mu \pi$ which amounts to a gauge fixing condition. This finally leads to

$$\mathscr{L} \supset \frac{1}{2}(\partial\sigma)^2 + \frac{1}{2}\left(g' \langle S \rangle\right)^2 Z'_\mu Z'^\mu + \frac{1}{2}\left(g'\sigma\right)^2 Z'_\mu Z'^\mu + g'^2 \sigma \langle S \rangle Z'_\mu Z'^\mu \tag{2.5}$$

We can identify $M_{Z'} := g' \langle S \rangle$ and we see that in this gauge the Z' boson has eaten the Nambu-Goldstone boson and gained an additional degree of freedom, namely it's longitudinal polarization. Analyzing the full Lagrangian one may worry this substitution is not helpful since it will introduce couplings between the Goldstone mode, which no longer has a kinetic term, and the charged fermions. Due to the lack of kinetic term, the field ceases to be a propagating degree of freedom and we may ignore its contributions; this justifies the transformation to unitary gauge.

The Faddeev-Popov method can allow one to see, somewhat more transparently, how this issue of Goldstone modes coupling to fermions is resolved. Here we choose our gauge fixing functional in such a way that the additional contribution to the Lagrangian density from integrating over the redundant degrees of freedom is given by [60]

$$\mathscr{L} \supset -\frac{1}{2\xi}\left(\partial^\mu Z'_\mu - \xi M_{Z'} \pi\right)^2 \tag{2.6}$$

After integration by parts this will remove the kinetic mixing that comes from expanding the bracketed gauge boson terms in Equation 2.4. After including the above gauge fixing term, resultant kinetic terms for Z' and π

in the Lagrangian will be of the form

$$\mathscr{L}_{kin} \supset \frac{1}{2}\left[(\partial\pi)^2 - \xi M_{Z'}^2 \pi^2\right] + \frac{1}{2} Z'_\mu \left[\eta^{\mu\nu}\partial^2 - \left(1 - \frac{1}{\xi}\right)\partial^\mu\partial^\nu + M_{Z'}^2\right] Z'_\nu \tag{2.7}$$

This leads to the following propagators for the Z' and the Goldstone mode

$$\langle 0|\, T\{Z'_\mu Z'_\nu\}\, |0\rangle = \frac{-i\eta_{\mu\nu} + i(1-\xi)\frac{k_\mu k_\nu}{k^2 - \xi M_{Z'}^2}}{k^2 - M_{Z'}^2} \tag{2.8a}$$

$$\langle 0|\, T\{\pi\pi\}\, |0\rangle = \frac{i}{k^2 - \xi M_{Z'}^2} \tag{2.8b}$$

This choice of gauge is known as R_ξ gauge and different choices of the parameter ξ define different gauges. In the limit of $\xi \to \infty$ unitary gauge is recovered and the mass of the Goldstone mode becomes infinite and it ceases to be a dynamical field. This is in agreement with the previous discussion. Calculations done in R_ξ gauge provide a useful consistency check to determine if any errors were made during a calculation because any physically observable quantity in the theory must be independent of the gauge parameter ξ. This cancellation is highly non-trivial and generally does not occur diagram by diagram.

2.2.2 Contributions to the Neutrino Mass Matrix

The mass matrix of the theory initially looks extremely restrictive, however, due to the Yukawa coupling with the Higgs singlet field and its acquisition of a vacuum expectation value additional mass terms are generated. We can then write the mass terms for the right-handed neutrinos as a mass matrix

written $\mathscr{L} \subset -\frac{1}{2} N_i M_{ij}^{(R)} N_j$. In the broken phase we may elect to write the singlet field in such a way as to emphasize the non-linear realization of the $U'(1)$ symmetry. To do this we define $m_{\mu,\tau} := \frac{1}{\sqrt{2}} g_{\mu,\tau} \langle S \rangle$ and express the right-handed mass matrix as

$$M_R = \begin{bmatrix} M_e & m_\mu & m_\tau \\ m_\mu & 0 & M \\ m_\tau & M & 0 \end{bmatrix} \tag{2.9}$$

notice that this matrix is controlled by four parameters. In the see-saw limit (see Section 1.4.3) the left-handed mass matrix is given by $M_L = \langle h \rangle^2 Y^T M_R^{-1} Y$ where $\langle h \rangle$ is the Standard Model Higgs' vacuum expectation value and Y is the matrix of Yukawa couplings which in our theory is diagonal in the flavour basis by virtue of our charge assignments. Applying the see-saw formula to the above right-handed mass matrix produces

$$M_L = \frac{\langle h \rangle^2}{M M_e - 2 m_\mu m_\tau} \begin{bmatrix} M & -m_\tau y_\mu y_e & -m_\mu y_\tau y_e \\ -m_\mu y_\mu y_e & \frac{m_\mu^2 y_\mu^2}{M} & \left(M_e - \frac{m_\mu m_\tau}{M} \right) y_\mu y_\tau \\ -m_\tau y_\tau y_e & \left(M_e - \frac{m_\mu m_\tau}{M} \right) y_\mu y_\tau & \frac{m_\tau^2 y_\tau^2}{M} \end{bmatrix} \tag{2.10}$$

The production of this mass matrix can be attributed to integrating out the right-handed neutrinos and writing down an effective theory. In this case more operators than the one above will be produced. The mass matrix, as it is written above, can be used to determine what the effective operators would look like before symmetry breaking. Note that $g_\mu S \to \left(m_\mu + \frac{1}{\sqrt{2}} g_\mu \sigma \right) e^{\pi / \langle S \rangle}$ so that we can make the substitution of $m_\mu \to g_\mu S$ in the above equation

and then subsequently break the symmetry. Correspondingly $m_\tau \to g_\tau S^\dagger$ so that terms involving the combination $m_\mu m_\tau$ have no coupling to the Goldstone modes. This results in the following "coupling matrix"

$$\frac{\langle h\rangle^2}{MM_e - 2g_\mu g_\tau |S|^2}\begin{bmatrix} M & -g_\tau y_\mu y_e S^\dagger & -g_\mu y_\tau y_e S \\ -g_\tau y_\mu y_e S^\dagger & \frac{g_\mu^2 S^2 y_\mu^2}{M} & \left(M_e - \frac{g_\mu g_\tau |S|^2}{M}\right) y_\mu y_\tau \\ -g_\mu y_\tau y_e S & \left(M_e - \frac{g_\mu g_\tau |S|^2}{M}\right) y_\mu y_\tau & \frac{g_\tau^2 \left(S^\dagger\right)^2 y_\tau^2}{M} \end{bmatrix} \tag{2.11}$$

One can then take $S \to \frac{1}{\sqrt{2}}(\langle S\rangle + \sigma)e^{i\pi/\langle S\rangle}$ and extract whatever couplings are of interest. To extract Feynman rules one must expand various functions as a Taylor series in the fields.

For the Goldstone modes this is fairly straightforward but for the gapped modes one must be careful since the denominator in front of this operator when expanded has terms of first and second order in the field σ. One way to avoid talking about couplings to the Goldstone modes is to work in Unitary Gauge however if one wishes to do a calculation in the broken phase in R_ξ gauge these couplings become very important as they are the manifestation of the longitudinal modes of the massive Z'.

2.2.3 Singlet Field in the Broken Phase

The breaking of the singlet field results in a modification of the scalar quanta's mass gap as well as inducing couplings that are not present in the unbroken phase. Taking the potential and expanding about the minimum

one finds that

$$V\left(|S|^2\right) \rightarrow \frac{\lambda_S}{2}\left(\frac{1}{2}\sigma^2 + \langle S\rangle\,\sigma\right)^2 = \frac{1}{2}\lambda_S\,\langle S\rangle^2\,\sigma^2 + \frac{3\lambda_S}{3!}\,\langle S\rangle\,\sigma^3 + \frac{3\lambda_S}{4!}\sigma^4 \quad (2.12)$$

The mass of the scalar excitation in the broken phase can be identified as $m_\sigma = \sqrt{\lambda_S}\,\langle S\rangle$. This result and the preceding discussion of couplings will not play a significant role in the rest of the discussion. If one wishes to take this model seriously and investigate its consequences these features would play and important role. For example the couplings resulting from the mass matrix can play an important role in the renormalization group flow of the Weinberg operator $L\tilde{H}L\tilde{H}$.

2.3 The Z' Progenitor Scenario Proposed by Shuve and Yavin 2014

The Dodelson Widrow proposal has been ruled out via galactic x-ray searches because the mixing with active neutrinos required to obtain the correct dark matter abundance predicts an excess of galactic x-rays that have not been observed (see Section 1.6). The progenitor scenario introduces a new mechanism by which sterile neutrinos could be produced which allows for a much smaller mixing angle to evade galactic x-ray bounds. This is because the model's production mechanism relies on physics beyond the Standard Model, and, as a result, is no longer constrained by the precision tests of the Standard Model.

The mixing results from mass terms that couple right-handed and left-handed particles to one another in the Lagrangian density. This mixing can be parameterized by an angle θ_m via the matrix equation

$$\begin{bmatrix} \nu_a \\ \nu_s \end{bmatrix} = \begin{bmatrix} \cos\theta_m & -\sin\theta_m \\ \sin\theta_m & \cos\theta_m \end{bmatrix} \begin{bmatrix} \nu_1 \\ \nu_2 \end{bmatrix} \tag{2.13}$$

Where the left hand side denotes active and sterile neutrinos in the flavour basis and ν_1 and ν_2 are the mostly active and mostly sterile mass eigenstates respectively. As such these are what represent propagating degrees of freedom. This scenario only includes one active and one sterile neutrino while our model contains three of each. These two pictures can be reconciled by thinking about integrating out the two heaviest sterile states and only considering the linear combination of active states that couple to the remaining sterile state. This is discussed in greater detail in Section 5.3.4.

High temperature effects modify the mixing angle resulting in a suppression which is given by the relationship below.

$$\sin^2 2\theta_m = \frac{\sin^2 2\theta_0}{\sin^2 2\theta_0 + [\cos 2\theta_0 + \Delta_R(k,T)]^2} \tag{2.14}$$

Where $\Delta_R(k,T)$ is related to the contribution to the neutrino self energy from vector-boson exchange [56, 57] (see Section 1.6).

The important feature here is that for $T \gtrsim 150\ \text{MeV}\left(\frac{m_s}{\text{keV}}\right)^{1/3}$ the mixing angle is heavily suppressed [7]. This allows for Z' decay to have no effect on dark matter production in early epochs of the universe while having significant

contributions after the universe cools below some critical temperature. This decay is mediated by $Z' \rightarrow \nu_a + \nu_a$ with one subsequent oscillation of $\nu_a \rightarrow \nu_2$ and another of $\nu_a \rightarrow \nu_1$ parametrically this results in the decay rate being proportional to $\sin^2\theta_m \cos^2\theta_m = 1/4 \sin^2 2\theta_m$. More careful analysis yields

$$\Gamma_{Z' \rightarrow \nu_2} = \frac{g' M_{Z'}}{12\pi} \frac{\sin^2 2\theta_m}{4} \tag{2.15}$$

in the limit where $\tan\theta_m << 1$ [7]. This allows one to calculate the relic abundances via the Boltzmann equation [61]. Shuve and Yavin found that the possibility of this mechanism is not excluded and calculated viable parameter combinations that can explain the observed dark matter energy density while simultaneously evading x-ray bounds [7]. The parameters of interest for their analysis were $M'_Z \approx$ MeV-GeV, $g' \approx 10^{-3} - 10^{-6}$, and $M_s \approx 1 - 100$ keV [7].

2.3.1 Restrictions on a new Z'

Introducing a new gauge group amounts to postulating a new force and with it a new Z' boson. This particle cannot have arbitrary properties and is subject to constraints both from collider searches and cosmological considerations.

It is worth noting the bound on the far left of Figure 2.1 from N_{eff}. This bound comes from Planck's measurement of the cosmic microwave background which is very sensitive to the number of neutrino species at neutrino

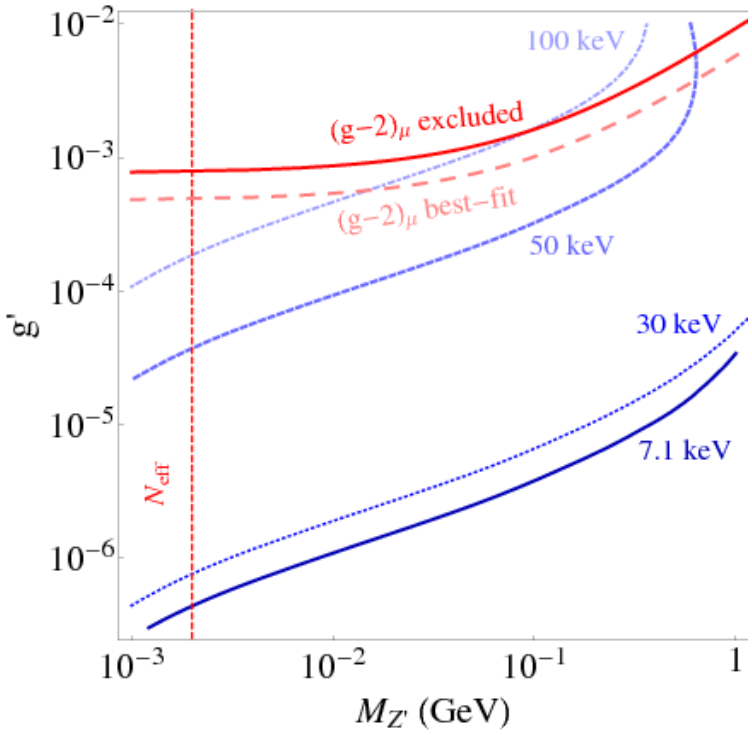

Figure 2.1: Plot showing contours in the $g' - M_{Z'}$ plane that fit to various masses of the sterile neutrino in the Z' progenitor scenario [7]. This plot was taken from Shuve and Yavin (2014)

freeze-out [14]. If $M_{Z'} \approx T_\nu^{fo}$, where T_ν^{fo} is the neutrino freeze-out temperature, the Z' will overpopulate the number of effective neutrino species via decay and the neutrino species will have no opportunity to equilibriate with the photon bath. If the decay occurs before neutrino freeze-out the number of neutrinos species can return to it's equilibrium distribution before freeze-out occurs and then the Plank measurement will be insensitive to this history.

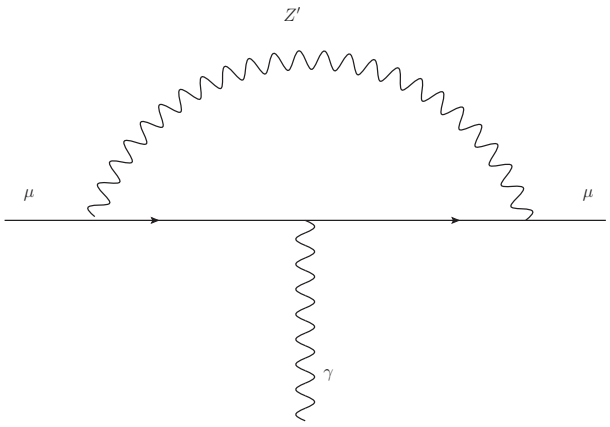

Figure 2.2: Z'contribution to the anomalous magnetic moment of the muon $(g-2)_\mu$

Collider searches can also place bounds on new Z' bosons however these colliders rely on hadronic and electron collisions [12, 62–64]. In our particular model of a gauged $L_\mu - L_\tau$ the Z' is completely hidden from these interactions. As a result the strongest bounds on Z' phenomenology comes from the muon's anomalous magnetic moment[65] and neutrino trident production [66]. The current measurement of the muon's anomalous magnetic moment $(g-2)_\mu$ is in disagreement with the Standard Model's prediction; this discrepancy is at the 3.3σ level [5]. The addition of a new Z' that couples only to the second and third generation leptons can remedy this situation without affecting the anomalous magnetic moment of the electron $(g-2)_e$. The contribution of the Z' to $(g-2)_\mu$ corresponds to the diagram shown in Figure 2.2. In the case where the Z' is massive this results in a

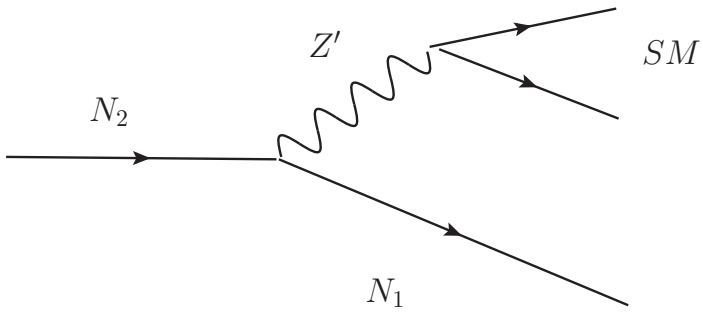

Figure 2.3: Decay mode of a heavier sterile N_2 into Standard Model particles and the dark matter candidate N_1 via a Z' interaction

correction to $(g-2)_\mu$ of [67]

$$\Delta(g-2)_\mu = \frac{\alpha'}{\pi}\int_0^1 \mathrm{d}x \frac{2m_\mu x^2\left(1-x^2\right)}{x^2 m_\mu + (1-x)M_{Z'}^2} \tag{2.16}$$

In the limit of $M_{Z'} << m_\mu$ this reduces to $\Delta(g-2)_\mu = \frac{\alpha'}{\pi}$ this is the familiar result from $Q.E.D$. In the opposite limit $M_{Z'} >> m_\mu$ the contribution is $\Delta(g-2)_\mu = \frac{\alpha'}{\pi}\frac{2m_\mu^2}{3M_{Z'}^2}$. This can been seen in the bounds in Figure 2.1 where the bound from $(g-2)_\mu$ is very flat until about 100 MeV $\approx m_\mu$. These measurements place bounds on the mass and coupling of the Z' because if the contribution from the Z' is too large its predictions will disagree with the measured value. If the contributions from the Z' do not account for the entire discrepancy from the Standard Model this does not rule out the model it just suggests that other physics beyond the Standard Model is the cause of this discrepancy.

Neutrino trident production is a rare process that occurs when neutrinos

scatter off of nuclei inelastically via the process $\nu + N \rightarrow \nu + \mu + \mu^+ + N$. In the standard model this process is mediated by the weak and electro-magnetic forces. With the inclusion of the Z' there are additional contributions [66]. Thus, agreement with the Standard Model predictions can place bounds on the Z' model.

2.4 Dark Matter Candidates in Our Model

The inclusion of sterile neutrinos in our model give multiple possible dark matter candidates. Due to the coupling between the various generations of right-handed neutrinos we should expect that the mixing between the generations could facilitate decay among the sterile neutrinos via a virtual Z' process such as the one shown in Figure 2.4. Dark matter must be stable and so the state which is a natural candidate for dark matter is the lightest of the sterile neutrino eigenstates.

The Z' scenario requires that the dark matter candidate couple to the new force only through kinetic mixing. This is because the scenario requires that the dark matter is produced non thermally and as such its production mechanism must be suppressed in the early epochs of the universe and subsequently turn on. Equation 2.3 allows for this to occur and relies on the fact that the dark matter is mostly composed of a sterile component. Additionally the zero temperature mixing must conform to x-ray bounds [11]. Thus to take advantage of the Z' progenitor scenario would require

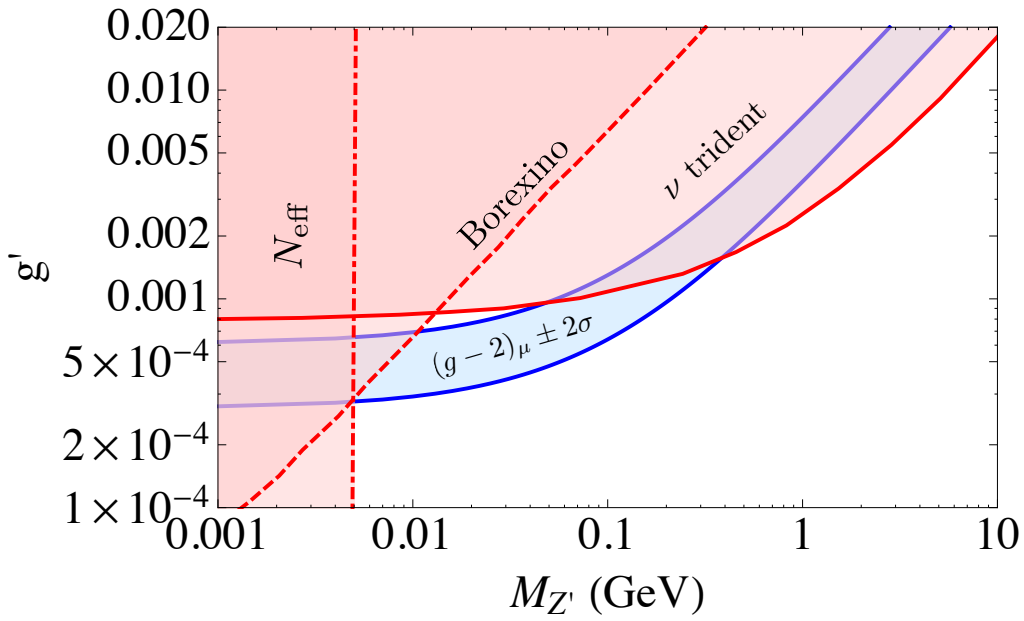

Figure 2.4: Bounds on a Z' coupling to the charge $L_\mu - L_\tau$ in the g' vs $M_{Z'}$ plane. Bounds from Borexino are sub-dominant to all other bounds. Neutrino trident production is the leading bound for $M_{Z'}$ larger than about 4 MeV. Plot produced by Brian Shuve. For a review of these bounds see ref. [12]

that this state be primarily N_e since the other two right-handed states are only sterile with respect to the Standard Model but couple directly to the Z'. As such for the purposes of the progenitor scenario we should identify the mass eigenstate which is most weakly coupled to the Z' as the dark matter.

One can then write down an effective theory containing only the lightest sterile eigenstate as a propagating degree of freedom and integrate out

the two heavier sterile states. This will leave an effective theory with a single right-handed neutrino state and a left-handed mass matrix generated by the two heavy right-handed states. One must insist on a right-handed mass spectrum that generates a mostly sterile (i.e. predominantly N_e in our model) lightest eigenstate. This is in correspondence with Equation 2.3 This scenario will be investigated in greater detail in Chapter 5.

CHAPTER 3

FITTING TO NEUTRINO DATA

Neutrino oscillation data offers the most stringent source of constraints for our model due to the high level of precision in solar, reactor and atmospheric neutrino oscillation experiments [68–71]. Generically any model with sterile neutrinos will generate neutrino masses, but due to the imposed symmetries of our model the right handed mass matrix is constrained with two of the entries vanishing. This manifests itself as a relationship between various entries of the left handed mass matrix which constrains the possible neutrino mass spectrum by having fewer than six free parameters to control the left handed mixing.

In the following chapter we will give conclusive evidence that without

additional dimension-five operators being added to the theory our model is incapable of generating the observed neutrino mass textures. This will be done in the see-saw limit which is justified for the combination of parameters of interest. First the mass matrix is conveniently parameterized. Next the set of all possible left handed mass matrices that could correspond to the observed neutrino phenomenology, in the CP conserving limit, is generated. Finally we will show that no element of this set can satisfy all of the relationships that exist between various entries in the parametrization of the mass matrix generated by our theory.

3.1 Mass Matrix Parameterization

Taking the inverse of the mass matrix expressed in Chapter 2 and multiplying on both sides by the Yukawa matrix we obtain the following expression for the left handed mass matrix

$$\frac{\langle h\rangle^2}{MM_e - 2m_\mu m_\tau}\begin{bmatrix} y_e^2 M & -m_\tau y_\mu y_e & -m_\mu y_\tau y_e \\ -m_\tau y_\mu y_e & \frac{m_\tau^2 y_\mu^2}{M} & \left(M_e - \frac{m_\mu m_\tau}{M}\right) y_\mu y_\tau \\ -m_\mu y_\tau y_e & \left(M_e - \frac{m_\mu m_\tau}{M}\right) y_\mu y_\tau & \frac{m_\mu^2 y_\tau^2}{M} \end{bmatrix} \tag{3.1}$$

where $\langle h\rangle$ is the Standard Model Higgs boson's vacuum expectation value.

Naively this matrix seems to be controlled by the set of Yukawa couplings, and the four entries in the right handed mass matrix for a total of seven independent degrees of freedom. However in reality the matrix can be

reduced to four independent parameters with one of these only controlling the overall mass scale.

$$M^{(L)} = \overline{\mathscr{M}} \begin{bmatrix} 1 & -\frac{r}{\mu} & -\frac{r^{-1}}{\mu} \\ -\frac{r}{\mu} & \frac{r^2}{\mu^2} & \frac{\mu\cdot\mu_e - 1}{\mu^2} \\ -\frac{r^{-1}}{\mu} & \frac{\mu\cdot\mu_e - 1}{\mu^2} & \frac{r^{-2}}{\mu^2} \end{bmatrix} \tag{3.2}$$

These variables are related to the original set of parameters by

$$r := \sqrt{\frac{m_\tau y_\mu}{y_\tau m_\mu}} \tag{3.3a}$$

$$\overline{m}_y := \sqrt{m_\mu m_\tau y_\mu y_\tau y_e^2} \tag{3.3b}$$

$$\mu := \frac{y_e^2 M}{\overline{m}_y} \tag{3.3c}$$

$$\mu_e := \frac{y_\mu y_\tau M_e}{\overline{m}_y} \tag{3.3d}$$

$$\overline{\mathscr{M}} := \mu \frac{\langle h \rangle^2}{\overline{m}_y} \frac{y_e^2 y_\mu y_\tau}{\mu\mu_e - 2} \tag{3.3e}$$

This reduction in the number of independent parameters is important because effectively we are attempting to fit to five pieces of information from neutrino oscillation data with only four parameters.

The two conditions that can be seen very transparently are the relationships between $M^{(L)}_{1j}$ and $M^{(L)}_{jj}$ for $j \in \{1,2\}$, namely that, after normalization, the square of the former is equal to the latter. This projects out two degrees of freedom compared to a general symmetric 3x3 matrix. We may define $\Omega := \frac{1}{M^{(L)}_{11}} M^{(L)}$ and then define $r_{jj} := \frac{\Omega^2_{1j}}{\Omega_{jj}}$. So we may check to see if any matrix

that can reproduce the measured neutrino textures can satisfy $r_{22} = r_{33} = 1$. These relationships are the result of parametrizing a symmetric 3×3 matrix (six independent entries) with only four independent parameters.

3.2 Generation of Possible Mass Matrices

To determine whether or not our model is capable of fitting to neutrino data there are a few possible strategies. We could begin by trying to extract the mixing angles from our theory as a function of the Lagrangian parameters. This strategy offers the advantage of having analytic control over the mixing angles however it is very costly in a computational sense. Another route one could elect to take would be to find solutions which fit to the mixing data in some coarse approximation and then perturb about these solutions. The disadvantage here is that due to the high precision measurements of the mixing data there is no guarantee that the coarse approximation is sufficiently close to a viable solution such that it is within reach of perturbation theory. Also can not conclusively prove that no solution exists using perturbation theory.

The final possible strategy abandons trying to solve for the mixing angles in terms of the given parameters and instead works to generate all possible mass matrices that could give the correct textures. These matrices would be written in the flavour basis and then compared to the parametrization given in Equation 3.1. This has the advantage of allowing one to calculate simple

analytic requirements for the generated mass matrices. For our theory these constraints are trivial and are just that $r_{22} = r_{33} = 1$. To construct all possible mass matrices we begin by noting that any neutrino mass matrix can be written

$$M^{(L)} = P^T diag(m_1, m_2, m_3) P \tag{3.4}$$

where P is the PMNS matrix. Now since we are interested in $\Omega := \frac{1}{M^{(L)}_{11}} M^{(L)}$ and we will be dividing by the magnitude of the first element so we may multiply the matrix by $\frac{1}{m_2}$ and still obtain the same Ω; this is equivalent to m_1 and m_3 being measured in units of m_2. It is convenient to use the second mass for normalization purposes since it is the only one of the three which is guaranteed to be non-zero in both the normal and inverted hierarchy.

We will allow the lightest mass m_ℓ to take on any value in the interval $[0, m_2]$. In the case of the normal hierarchy this is m_1 and for the inverted hierarchy this is m_3. The remaining mass which has not been fixed will be determined by the relationships between the mass squared differences. The remaining degrees of freedom are discreet and correspond to the possibility of any of the masses being negative.

We partition the set of possible matrices in the following way. First distinguish between the normal and inverted hierarchies as they have different mixing angles. Next within these sets we distinguish between the cases where either all three masses are positive, or where one of the masses is

negative resulting in a total of four cases (one for each negative mass). This is exhaustive since all other combinations can be obtained via scalar multiplication of M^L which will be cancelled in the normalization of Ω.

This leaves us with eight sets of matrices, with either m_1 or m_3 undetermined depending on the hierarchy of interest. We then have a computer program run through all possible values of the lightest mass and generate the various possible matrices. Each of these matrices' r_{22} and r_{33} values are then calculated and plotted for the various masses.

As can be seen from Figures 3.1 and 3.2 at no point do both conditions become simultaneously satisfied nor do they come with in any reasonable neighbourhood of being simultaneously satisfied (all three plotted lines intersecting i.e. $r_{22} = r_{33} = 1$. For further discussion see Appendix B.

One may subsequently be tempted to wonder how sensitive the matrices produced from the experimental data are to changes in the mixing angles and mass spectra. Due to the high precision of the measurements made the sensitivity to modification of measured parameters at the 2σ level is small and is orders of magnitude smaller than the discrepancy between the model and observation.

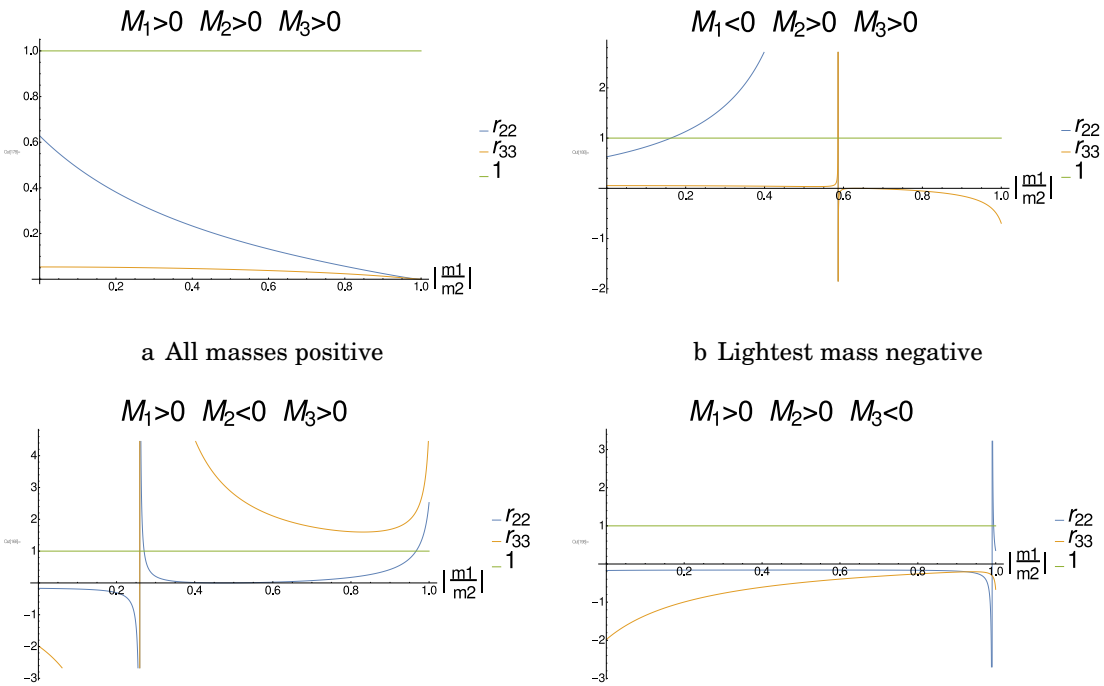

a All masses positive

b Lightest mass negative

c Middle mass negative

d Heaviest mass negative

Figure 3.1: Possible normal hierarchy mass matrices' r_{22} and r_{33} generated by taking central fit values for the PMNS matrix [8] and rotating all possible mass spectra that conform to the data for the normal hierarchy into the flavour basis

3.3 Successes of this Minimal Model

Although we have shown that this model is inconsistent with observed neutrino phenomenology the features it produces are very similar to what is observed in nature. Due to the high level of precision present in modern measurements of neutrino phenomenology the model is excluded however it

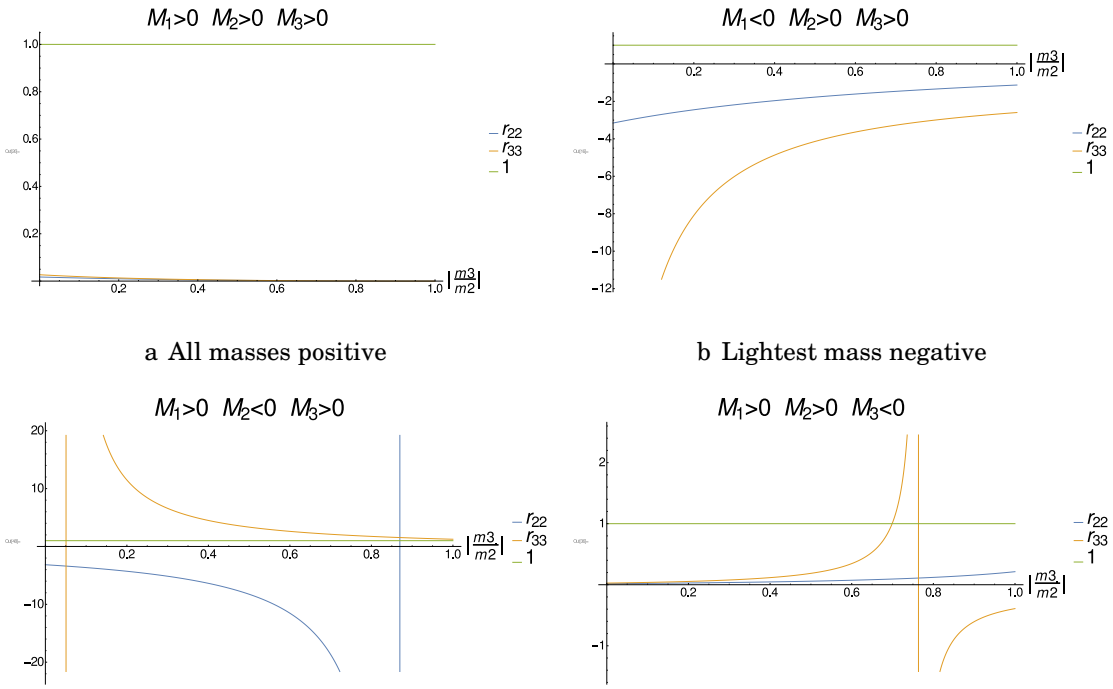

a All masses positive

b Lightest mass negative

c Middle mass negative

d Heaviest mass negative

Figure 3.2: Possible Inverted hierarchy mass matrices' r_{22} and r_{33} generated by taking central fit values for the PMNS matrix [8] and rotating all possible mass spectra that conform to the data for the inverted hierarchy into the flavour basis

is able to succeed to within about $25-30\%$ for all of the values of $\sin^2\theta_{ij}$. The two conditions ($r_{22}=r_{33}=1$) manifest themselves as tension between θ_{13} and θ_{12} while θ_{23} is easily accommodated by an approximate $\mu\leftrightarrow\tau$ exchange symmetry. As you can see in Table 3.3 we are able to match to two of the three mixing angles and achieve the correct ratio of mass squared

Quantity	Prediction	nu-Fit value	% Difference	σ Discrepancy
$\Delta m^2_{13}/\Delta m^2_{12}$	32.40	32.44	0.1%	0.13σ
$\sin^2\theta_{13}$	0.0198	0.0218	9.2%	2.00σ
$\sin^2\theta_{12}$	0.296	0.304	2.7%	0.68σ
$\sin^2\theta_{23}$	0.329	0.452	27.2%	4.40σ

Table 3.1: Comparison of minimal model's predicted neutrino texture for $r = 0.8212$, $\mu = -0.61$, $\mu_e = 0.75$. This texture is in the normal hierarchy and so $\sin^2\theta_{23}$ is the appropriate value. All neutrino data is taken from [8]

differences however the precision measurements rule out the predicted neutrino texture conclusively despite matching to within about 25%. A similar fit can be made in which θ_{12} is fit to within less than 1σ however this comes at the cost of a near vanishing θ_{13}.

CHAPTER 4

MODIFYING THE MODEL

The inability of our model to fit neutrino oscillation data mandates the inclusion of additional degrees of freedom if our extension of the Standard Model is to explain the neutrino oscillation data. These additional degrees of freedom could manifest themselves as additional fields in the model, or as higher dimensional operators with the same field content.

These two possibilities are united via the language of effective field theory. The inclusion of additional matter content can generate higher dimensional operators in the low energy effective theory. As a result we can investigate the effects of various higher dimensional operators at low energies while

remaining agnostic as to their origin in the ultraviolet.

We have already considered all operators of dimension four or less, however we know that operators of higher dimensionality are suppressed by appropriate powers of some cut off. So to leading order we should only concern ourselves with operators of dimensionality less than or equal to five.

4.1 Possible Dimension-Five Operators

If we ignore Weinberg type operators the set of possible dimension-five operators that concern the generation of neutrino masses will have to contain at least one of the sterile fields N_i. As a result this must couple to at least one other Weyl spinor to achieve Lorentz invariance. This gives us the choice of either another sterile state, or the Standard Model leptons. One class of operators corresponds to the former, and one to the latter. I will refer to these as mass-inducing and Yukawa-inducing operators respectively.

The mass operators, at this point, are composed of only two Weyl spinors and so can accommodate two additional powers of energy. The only possible field which can achieve this while maintaining Lorentz invariance is the $SU(2)$ singlet scalar field S, which will come in two powers. This allows us to include the operators

$$\frac{\delta M_\mu}{\langle S \rangle^2} N_\mu N_\mu S^2 \tag{4.1a}$$

$$\frac{\delta M_\tau}{\langle S\rangle^2} N_\tau N_\tau \left(S^\dagger\right)^2 \tag{4.1b}$$

where N_μ and N_τ are the right-handed neutrinos charged under the $U'(1)$ symmetry and δM_μ and δM_τ are couplings with mass dimension one.The ratio $\delta M_{\mu,\tau}/\langle S\rangle$ controls the strength of these dimension-five operators. These operators will modify the right-handed mass matrix; this is the root of the mass operator nomenclature. In principle there is also the operator $N_e N_e S S^\dagger$, however this can be captured by a redefinition of M_e.

Due to the $SU(2)$ structure of the left-handed leptons we must include couplings that include both the Higgs doublet and the lepton doublet. Since we are interested in operators that will modify the left-handed mass matrix, we must couple to the right-handed neutrinos as well. This leaves four possible operators; these are called Yukawa-inducing operators

$$\frac{Z_\mu}{\langle S\rangle} L_e \tilde{H} N_\mu S \tag{4.2a}$$

$$\frac{Z_\tau}{\langle S\rangle} L_e \tilde{H} N_\tau S^\dagger \tag{4.2b}$$

$$\frac{\chi_\tau}{\langle S\rangle} L_\tau \tilde{H} N_e S^\dagger \tag{4.2c}$$

$$\frac{\chi_\mu}{\langle S\rangle} L_\mu \tilde{H} N_e S \tag{4.2d}$$

As these operators have been written their inclusion in the mass and Yukawa matrices respectively is manifest after setting the singlet scalar field equal to its vacuum expectation value.

It is worth pausing and qualitatively discussing the effects of these operators. The mass operators will result in a modified right-handed mass matrix. As a result its inverse will have some additional degrees of freedom and the constraints on the left-handed mass matrix will be relaxed.

The Yukawa-inducing operators that couple L_e to N_μ and N_τ allow the generation of a 3x3 left-handed mass matrix, even for the case of a vanishing y_e. The operators that couple N_e to Standard Model leptons, conversely, induce a coupling of N_e to the Standard Model even in the limit of a vanishing y_e. We may therefore think of the $Z_{\mu,\tau}$ operators as a way to produce acceptable neutrino textures without coupling N_e to the Standard Model while the $\chi_{\mu,\tau}$ operators induce additional coupling between N_e and the Standard Model; this will be important when we discuss dark matter.

4.2 Consequences of Mass-Inducing Operators

The inclusion of the mass-inducing operators results in a new right-handed mass matrix. After the singlet state acquires a vacuum expectation value this matrix can be written

$$M_R = \begin{bmatrix} M_e & m_\mu & m_\tau \\ m_\mu & \delta M_\mu & M \\ m_\tau & M & \delta M_\tau \end{bmatrix} \tag{4.3}$$

(see Section 2.2.2)After applying the see-saw relation with a diagonal Yukawa matrix the resultant left-handed mass matrix for $\delta M_\tau = 0$ is given by

$$M_L = \overline{\mathscr{M}} \begin{bmatrix} 1 & -\frac{r}{\mu} & -\frac{r^{-1}}{\mu} + \delta_\mu \frac{r}{\mu} \\ -\frac{r}{\mu} & \frac{r^2}{\mu^2} & \frac{\mu \cdot \mu_e - 1}{\mu^2} \\ -\frac{r^{-1}}{\mu} + \delta_\mu \frac{r}{\mu} & \frac{\mu \cdot \mu_e - 1}{\mu^2} & \frac{r^{-2}}{\mu^2} - \delta_\mu \frac{\mu_e}{\mu} \end{bmatrix} \tag{4.4}$$

These parameters are the same as those introduced in Chapter 3 (with the additional contribution from δM_μ), and are related to the original set of parameters by :

$$r := \sqrt{\frac{m_\tau y_\mu}{y_\tau m_\mu}} \tag{4.5a}$$

$$\overline{m}_y := \sqrt{m_\mu m_\tau y_\mu y_\tau y_e^2} \tag{4.5b}$$

$$\mu := \frac{y_e^2 M}{\overline{m}_y} \tag{4.5c}$$

$$\mu_e := \frac{y_\mu y_\tau M_e}{\overline{m}_y} \tag{4.5d}$$

$$\overline{\mathscr{M}}_\mu := \frac{\langle h \rangle^2}{\overline{m}_y} \frac{y_e^2 y_\mu y_\tau}{\mu \mu_e - 2 + \delta_\mu r^2} \mu \tag{4.5e}$$

$$\delta_\mu := \frac{\delta M_\mu y_\tau}{M y_\mu} \tag{4.5f}$$

The limit in which $\delta M_\mu = 0$ and $\delta M_\tau \neq 0$ can be obtained by exchanging the μ and τ indices, and taking $r \to r^{-1}$ on any of the quantities contained in the definitions of δ_μ and $\overline{\mathscr{M}}_\mu$.

Table 4.1 shows that all of the dimensionless parameters defined by Equation 4.5 that are required to fit the neutrino textures are within two orders

of magnitude of unity. This condition is enough to obtain rough parametric dependence of various parameters to within two orders of magnitude.

This matrix differs from the mass matrix of our previous theory in that we no longer have the condition that $\Omega_{13}^2 = \Omega_{33}$ ($\Omega_{12}^2 = \Omega_{22}$) for a non-zero δM_μ (δM_τ). Provided the other dimension-five operator vanishes, the remaining constraint remains so we may make use of the data from Figure 3.1 and Figure 3.2 to determine which regions of parameter space can be fit with only one of these operators.

We see that there are single points of intersection between r_{22} and the horizontal line set equal to unity in Figures 3.1b,3.1d, 3.2d and two points of intersection in Figure3.1c. In Figure 3.1b there is also one mass combination that could be fit by a non-zero value of δM_τ. The matrices corresponding to these points of intersection can then becompared to the parametrization in Equation 4.2, and the parameters that fit to this matrix can be extracted.

4.2.1 Finding the Model Parameters

We have identified matrices that our theory can parametrize at tree level and that agree with experimental neutrino textures . Now we must develop a procedure to extract the Lagrangian parameters which yield a mass spectrum that agrees with experiment.

Since we are fitting in flavour space, this procedure only requires that we

equate each entry of the generated mass matrix with our matrix parametrization. This will allow us to determine μ, μ_e, δM_μ, and r. The overall mass scale is not fixed by experiment, but is bounded from above by cosmological considerations [14], and from below by Δm^2_{13} [8].

Due to the conventional positivity of the Yukawa couplings, M_e, m_μ, and m_τ, we can rule out any solutions that require either μ_e or r^2 to be negative. In contrast, we can say nothing about the phase of either δ_μ or μ, which is in one to one correspondence with the unconstrained phases of δM_μ and M. The possible combinations of parameters which fit to the central values of the neutrino parameters from nu-Fit are given in Table 4.1.

Note that all of the parameters are approximately of order one. We must be careful to ensure that our effective field theory picture is self consistent. We would naively expect $\delta M_\mu < M$ due to energy scale suppression, however some fits have $\delta_\mu > \mu$ which would require that $y_\tau >> y_\mu$ to maintain our naive assumption.

All of the fits presented in Table 4.1 have all of the parameters approximately equal to one with the exception of the first line where $\mu \approx 0.05$, however this is still only about an order of magnitude discrepancy. The fact that all of the parameters need to contribute significantly to the mixing is an important feature of the model and will be expanded upon in Chapter 5.

Hierarchy	$\frac{m_\ell}{m_2}$	μ	μ_e	δ_μ	r	$\overline{\mathscr{M}}$ (eV)
Normal	-0.271	0.0471	1.51	9.45	0.823	$6.43 \cdot 10^{-5}$
Normal	-0.967	-0.741	0.641	-0.380	0.976	0.0135
Normal	-0.162	0.262	1.76	1.87	0.786	0.00272
Normal	0.995	-4.72	4.99	-0.194	1.04	0.0803
Inverted	-0.704	4.70	-3.81	0.319	0.914	0.0117

Table 4.1: Parameter values for mass-inducing operators that fit to the data. $\frac{m_\ell}{m_2}$ is the ratio of the lightest mass to m_2

4.3 Yukawa-Inducing Operators

4.3.1 Motivation

After symmetry breaking the Yukawa-inducing operators of interest exclusively couple first-generation lepton fields to second-generation lepton fields. We may therefore distinguish between two classes of operators. Those that couple L_e to sterile fields and those that couple N_e to Standard Model states as was done in Equation 4.1.

We have just found that by introducing dimension-five operators into the mass matrix we can fit to the central values of neutrino data. Since mass-inducing operators are sufficient one may be inclined to ask what the purpose of discussing these Yukawa-inducing operators is?

This thesis concerns the interplay of neutrino oscillations and the Shuve-Yavin Z' progenitor scenario, therefore the ability for our model to conform to bounds from dark matter is of great significance. These bounds will be discussed in the next chapter however, heuristically we can expect any coupling to the Standard Model from a dark matter candidate to be potentially problematic because this will affect the mixing angle constrained by galactic x-ray searches [11].

We would naturally identify the lightest sterile state as a potential dark matter candidate, therefore we need only consider one linear combination of the sterile fields (namely that which has the smallest mass). For the Z' scenario the sterile state is required to be uncharged under $L_\mu - L_\tau$. This naturally suggests that N_e would need to compose the majority of the dark matter candidate.

As a result it would be helpful to see if for certain additional operators the correct neutrino phenomenology could be obtained even in the limit of an entirely decoupled dark matter candidate which would be composed mostly of N_e. This is related to the fact that the mixing angle θ_m in the Shuve Yavin progenitor scenario is constrained by galactic x-ray searches. To exist within viable parameter space our dark matter candidate must be sufficiently decoupled so as not to produce x-ray abundances in excess of the bounds set by astronomers [11].

Any operator that connects N_e to Standard Model neutrinos will facilitate decay via the channel $N \to \nu + \gamma$ (see Figure 1.6). Operators which couple N_e to the Standard Model are not of interest as they will only serve to enhance the decay rate. Thus, we are interested in operators which couple N_μ or N_τ to L_e; these are defined by Equation 4.2a and 4.2b.

We would therefore like to see if, in the absence of any other non-zero dimension-five operators, Z_μ and Z_τ can satisfy the neutrino phenomenology, even in the limit of $y_e = 0$.

4.3.2 Resultant Left-Handed Mass Matrix

In this case the right-handed mass matrix, and consequently its inverse, is unaffected by the additional Yukawa-inducing operators. After expanding the see-saw formula. however, we see a markedly different left-handed mass matrix due to the modified Yukawa matrix. The parametrization used previously involved the quantity $\overline{m}_y \propto y_e$. But since we are taking $y_e = 0$ this quantity is not particularly useful. It turns out that the matrix can be parameterized more conveniently by the variables:

$$X_\mu = \frac{Z_\mu}{y_\mu} \tag{4.6a}$$

$$X_\tau = \frac{Z_\tau}{y_\tau} \tag{4.6b}$$

$$\kappa_\mu = \frac{m_\mu}{\sqrt{M_e M}} \sqrt{\frac{y_\tau}{y_\mu}} \tag{4.6c}$$

$$\kappa_\tau = \frac{m_\tau}{\sqrt{M_e M}} \sqrt{\frac{y_\mu}{y_\tau}} \tag{4.6d}$$

$$\overline{\mathscr{M}}_Y = \frac{\langle h \rangle^2}{M} \frac{y_\mu y_\tau}{1 - 2\kappa_\mu \kappa_\tau} \tag{4.6e}$$

Using these relations the left-handed mass matrix can be written as

$$M_L = \overline{\mathscr{M}}_Y \begin{bmatrix} X_\mu^2 \kappa_\tau^2 + X_\tau^2 \kappa_\mu^2 + 2\left(1 - \kappa_\mu \kappa_\tau\right) X_\mu X_\tau & \bullet & \bullet \\ \kappa_\tau^2 X_\mu + \left(1 - \kappa_\mu \kappa_\tau\right) X_\tau & \kappa_\tau^2 & \bullet \\ \kappa_\mu^2 X_\tau + \left(1 - \kappa_\mu \kappa_\tau\right) X_\mu & 1 - \kappa_\mu \kappa_\tau & \kappa_\mu^2 \end{bmatrix} \tag{4.7}$$

where the dots reference the symmetry of the mass matrix. The parameters that fit experimental data all predict the lightest neutrino to have zero mass. This is not surprising since generically, models with right-handed neutrinos require at least one right-handed neutrino for every massive left-handed neutrino [58]. N_e is entirely decoupled from the Standard Model particles at tree level. This implies that we effectively only have two sterile neutrinos for the purposes of left-handed mass generation.

Table 4.2 shows multiple different solutions that reproduce the correct neutrino phenomenology. Note that there are fewer solutions than in Table 4.1. This is because, with the lightest mass set to zero, the number of possible sign combinations for the matrices reduces from two to four, since negative and positive m_ℓ are indistinguishable in the limit where $m_\ell \to 0$.

Note that once again all parameters of interest are approximately of order one. In this case having $Z \approx y$ is somewhat more palatable than $\delta M_\mu \approx M$ since nothing forbids arbitrarily small Yukawa couplings.

Hierarchy	$\frac{m_\ell}{m_2}$	X_μ	X_τ	κ_μ	κ_τ	$\overline{\mathscr{M}}_Y$ (eV)
Normal	0	0.595	−0.339	0.694	0.630	$6.06 \cdot 10^{-3}$
Normal	0	0.595	−0.339	0.787	0.715	$6.06 \cdot 10^{-3}$
Inverted	0	−5.09	−4.34	5.17	4.43	$1.93 \cdot 10^{-4}$
Inverted	0	−5.09	4.34	1.13	0.320	$2.46 \cdot 10^{-3}$

Table 4.2: Parameter values for Yukawa-inducing operators that fit to the data. $\frac{m_\ell}{m_2}$ is the ratio of the lightest mass to m_2.

We have shown that for both mass and Yukawa-inducing operators the correct neutrino phenomenology can be generated. In the case of the Yukawa-inducing operators this was done in the limit where $y_e = 0$ with no dimension-five operators coupling N_e to Standard Model leptons. As a result we say N_e is entirely decoupled.

4.4 Weinberg-Inducing Operators

If we wish to remain entirely agnostic we should also include the dimension-five Weinberg-inducing operators that couple Standard Model leptons to other Standard Model leptons. These are

$$\mathscr{W}_e \left(L_e \tilde{H}\right)\left(L_e \tilde{H}\right) \tag{4.8a}$$

$$\mathscr{W}_{\mu,\tau} \left(L_\tau \tilde{H}\right)\left(L_\mu \tilde{H}\right) \tag{4.8b}$$

These operators result in direct contributions to the neutrino mass matrix. Since we are interested in whether or not the progenitor scenario and neutrino textures can be explained in a unified frame work these operators are not of particular interest to us. It should be noted that these Weinberg-inducing operators would modify the conditions that Ω has to obey from $r_{22} = r_{33} = 1$ to the less restrictive $r_{22} = r_{33}$.

4.5 A Comment on the Mass Scale

By matching the model's neutrino textures to the experimentally measured neutrino textures we have obtained various predictions for the overall mass scale. This can be probed by measuring anisotropies in the cosmic microwave background [14] or by searching for neutrinoless double beta decay [72]. The former is able to constrain the sum of all of the neutrino masses [14] while the latter can set bounds on one entry in the left-handed neutrino mass matrix as it is written in the flavour basis.

To understand the final comment it is useful to understand what neutrinoless double beta decay is. Beta decay is the name given to the process $N \to P + e + \overline{\nu}_e$ where N is a neutron, P is a proton, e and electron, and $\overline{\nu}_e$ is an anti-neutrino. Neutrinoless double beta decay is a much rarer process given by $2N \to 2P + 2e$. This process violates lepton number and observing its signal is direct evidence of a Majorana mass for the Standard Model neutrinos [73]. The matrix entry this process is sensitive to is $M^{(L)}_{11} \equiv M^{(L)}_{ee}$.

This can be understood on the level of partons by the diagram in Figure 4.1.

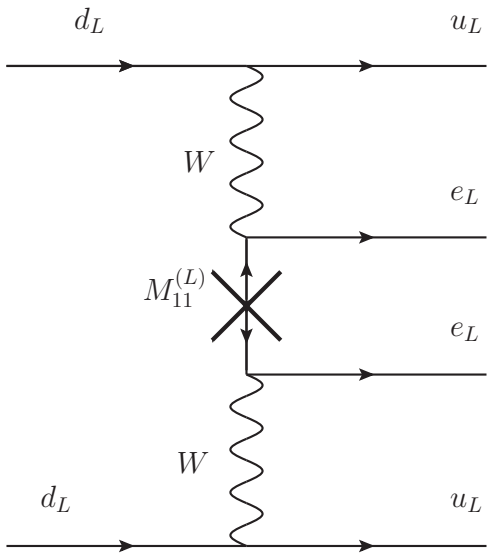

Figure 4.1: Parton level diagram contributing to neutrinoless double beta decay. This diagram is written using two component spinor techniques where the arrows track chiral charge. We see that to get two outgoing electrons that couple to the weak charged-current we need a Majorana mass term M_{11}.

The bounds from cosmology and neutrinoless double beta decay experiments are shown in Figure 3 of [72]. The mass scales we found satisfy the experimental requirements however there is no distinctive signal of this theory in neutrinoless double beta decay experiments assuming we consistently include all dimension five operators. Even just considering the one mass-

inducing operator, and the two Yukawa-inducing operators we have found multiple solutions for the normal, and inverted hierarchies. Were we to consider these operators simultaneously there would be further solutions.

It should be emphasized that in the case of the mass-inducing analysis the parameter $\overline{\mathscr{M}}$ is exactly M_{11}. In the case of the Yukawa-inducing operators $\overline{\mathscr{M}}_Y$ must be multiplied by the first entry in the matrix in Equation 4.7. This number turns out to always be some number that is very close to unity and because $\overline{\mathscr{M}}_Y$ is less than 0.01 eV the non observation of neutrinoless double beta decay is consistent with our model.

The model's predictions satisfy the requirements of cosmic microwave background measurements and neutrinoless double beta decay searches. There is no "smoking gun" of our model that can be found in neutrinoless double beta decay experiments.

4.6 A Quick Summary

We have found that by augmenting our minimal model we are able to fit to the best fit parameters in the literature for neutrino mixing. We have found that this can be achieved in two distinct non trivial ways in an effective field theory frame work: via mass-inducing and Yukawa-inducing operators.

The successful fits all had the parameters defined by Equations 4.5 and

4.6 to be order one. We argue that the Yukawa-inducing operators being comparable to the Yukawa couplings of the theory is more easily accommodated within the language of effective field theory than the mass-inducing operators being on the same order as the Majorana masses as is suggested by the order one parametrics in Table 4.1.

CHAPTER 5

DARK MATTER VIABILITY AND X-RAY CONSTRAINTS

In the previous section we succeeded in showing that both mass and Yukawa-inducing operators (defined by Equation 4.5 and 4.6 respectively) are sufficient additions to the model to fit to the observed neutrino phenomenology. What remains to be seen is the capacity of these models to account for dark matter phenomenology without violating bounds from galactic x-ray searches.

In this chapter we will examine the relative sizes of the various Lagrangian parameters that are implied by the neutrino data. We will then see that the parametric dependence that is required to satisfy the conditions of the

Z' progenitor scenario cannot be achieved while simultaneously satisfying galactic x-ray search bounds.

5.1 Mixing angles in the See-Saw Limit

As reviewed in the introduction, the see-saw mechanism involves the coupling of a set of massless Weyl spinors to a set of massive Weyl spinors with characteristic mass scale M via a Dirac mass term $m^{(D)}$. The see-saw limit is defined by the criterion $m^{(D)} << M$. We would ultimately like to find a basis in which the mass couplings are diagonal to isolate propagating degrees of freedom. For n massless fermions and m massive fermions this amounts to diagonalizing the following matrix.

$$\begin{bmatrix} 0 & m^{(D)}_{m\times n} \\ m^{(D)}_{n\times m} & M_{m\times m} \end{bmatrix} \tag{5.1}$$

In the case of $n = m = 1$ this can be understood easily the context of perturbation theory. The leading order correction to the mass of the massless state is $\frac{m^{(D)}}{M}$, and the first-order eigenstates are given by $(1, -\frac{m^{(D)}}{M})^T$ and $(\frac{m^{(D)}}{M}, 1)^T$. If we parametrize the rotation matrix that diagonalizes our states by the standard convention we can equate to first-order

$$\begin{bmatrix} \cos\theta_m & \sin\theta_m \\ -\sin\theta_m & \cos\theta_m \end{bmatrix} \approx \begin{bmatrix} 1 & \theta_m \\ -\theta_m & 1 \end{bmatrix} = \begin{bmatrix} 1 & \frac{m^{(D)}}{M} \\ -\frac{m^{(D)}}{M} & 1 \end{bmatrix} \tag{5.2}$$

So, we see that in the see-saw limit, $\sin\theta_m \approx \theta_m = \frac{m^{(D)}}{M}$. This means that bounds from x-ray searches, which are quoted in terms of $\sin^2\theta_m$, can be

translated into bounds on the relative size of the Dirac mass compared to the Majorana mass scale (provided the see-saw approximation is valid).

5.2 Requirements for Z' Progenitor Dark Matter

The Z' progenitor decay scenario is reliant on the production of the dark matter candidate being dominated by the kinetic mixing of a sterile state with vanishing charge and an active state with non-zero charge under the $U'(1)$ gauge group. In our model we seek some linear combination of N_e, N_μ, and N_τ to be our dark matter candidate. Any amount of N_μ or N_τ will result in some coupling to the Z' . Therefore this coupling must be sufficiently suppressed. This is equivalent to saying that the lightest eigenstate of the right-handed mass matrix is almost entirely N_e. To achieve this one requires that $\delta M \approx M >> m_\mu \approx m_\tau >> M_e$. This can be understood using perturbation theory. Suppose $\frac{m_{\mu,\tau}}{M} \approx \epsilon$ and $\frac{M_e}{M} \approx \epsilon^2$ while $\delta M_\mu \approx M$. We can then write the right-handed mass matrix as

$$M_R = M\left(\begin{bmatrix} 0 & 0 & 0 \\ 0 & \# & 1 \\ 0 & 1 & 0 \end{bmatrix} + \epsilon \begin{bmatrix} 0 & \# & \# \\ \# & 0 & 0 \\ \# & 0 & 0 \end{bmatrix} + \epsilon^2 \begin{bmatrix} \# & 0 & 0 \\ 0 & 0 & 0 \\ 0 & 0 & 0 \end{bmatrix}\right) \tag{5.3}$$

Where all of the # stand for $\mathcal{O}(1)$ numbers. We can see that at zeroth-order in perturbation theory the eigenstates are given by $(1,0,0)^T$, and two orthogonal linear combinations of $(0,1,-1)^T$ and $(0,1,1)^T$. The former

has zero mass and the latter two states have masses on the order of M. The effects of the perturbations are to mix the unperturbed states (this effect appears at first-order) and to shift the masses of the unperturbed states. This happens at second-order in ϵ since the diagonal perturbation is $\mathcal{O}(\epsilon^2)$ and the off diagonal perturbation, which only affects eigenvalues at second-order, is $\mathcal{O}(\epsilon)$.

This implies that the mass of the lightest state will be of order $M\epsilon^2 = M\left(\frac{M_e}{M}\right) = M_e$ and that the N_μ and N_τ content of this state will be on the order of ϵ. Thus, provided ϵ is sufficiently small, we will have a lightest right-handed neutrino with minimal N_μ and N_τ content and a mass that is set by the parameter M_e. Other possible hierarchies of parameters in the mass matrix can give a sterile state but it will not be the lightest of the three without excessive tuning.

5.3 A Single-Sterile Effective Theory

Our discussion of mixing angles in Section 5.1 was most transparent when we discussed the case of a single sterile state mixing with a single active state. This is because, when more species are introduced, additional angles must also be introduced. We would therefore like some simplified theory in which our dark matter candidate mixes with some linear combination of Standard Model neutrinos such that the mixing can be parameterized by a single angle.

It is convenient to integrate out the heavy sterile states and produce an effective theory in which the only sterile state is the dark matter candidate. To do this we must diagonalize the right-handed mass matrix to find the mass basis; this will be composed of three states: N_1, N_2, and N_3. We may then express our Lagrangian density in this new basis — let us call this $\mathscr{L}(N_1, N_2, N_3)$ where any other field dependence has been suppressed for brevity's sake.

N_1 is the lightest eigenstate and is to be identified as our dark matter candidate. We wish to find an effective Lagrangian density, $\mathscr{L}_{eff}(N_1)$, that accurately describes the low-energy physics with no mention of the two heavier mass eigenstates N_2 and N_3. To obtain an effective theory with only one sterile state, we set N_2 and N_3 equal to their classical equations of motion in the low-energy limit (see Section 1.1).

This will result in an effective Lagrangian density that contains the following terms

$$\mathscr{L}_{eff} \supset -\frac{1}{2}M_1 N_1 N_1 + N_1 \tilde{H}\left(y'_e L_e + y'_\mu L_\mu + y'_\tau L_\tau\right) - \frac{1}{2}M'_{ij} L_i L_j \tag{5.4}$$

where M' is the mass matrix obtained by integrating out the two heavy sterile states and the set of y' couplings are Yukawa couplings between N_1 and the Standard Model leptons induced by kinetic mixing. The linear combination of Standard Model neutrinos in brackets, up to a normalization factor, will be denoted by ν_Σ. We may then parametrize the mixing between

this active state ν_Σ and N_1 by a single mixing angle θ_m.

5.3.1 Zeroth-Order Result

Due to the necessary hierarchy of parameters we may find M_1, M_2, and M_3 (corresponding to N_1, N_2 and N_3) in perturbation theory as discussed in Section 5.2. Quantities Q which are determined to n^{th} order in perturbation theory will be denoted $Q^{(n)}$ such that $Q = \sum \epsilon^n Q^{(n)}$. So our first step is to solve the zeroth-order mass matrix's spectrum. Explicitly the right-handed mass matrix is given by

$$M_R = M\left(\begin{bmatrix} 0 & 0 & 0 \\ 0 & \frac{\delta M_\mu}{M} & 1 \\ 0 & 1 & 0 \end{bmatrix} + \frac{\sqrt{m_\mu m_\tau}}{M}\begin{bmatrix} 0 & \rho & \rho^{-1} \\ \rho & 0 & 0 \\ \rho^{-1} & 0 & 0 \end{bmatrix} + \frac{M_e}{M}\begin{bmatrix} 1 & 0 & 0 \\ 0 & 0 & 0 \\ 0 & 0 & 0 \end{bmatrix}\right) \tag{5.5}$$

where $\rho = \sqrt{m_\mu/m_\tau}$ and keeping in mind that $\frac{\sqrt{m_\mu m_\tau}}{M}$ is $\mathcal{O}(\epsilon)$ and $\frac{M_e}{M}$ is $\mathcal{O}(\epsilon^2)$.

This is readily achieved exactly for arbitrary values of δM_μ, but it will be sufficiently illustrative, and markedly simpler, to work in the limit of $\delta M_\mu = 0$. In this case the spectrum is given by eigenvalues $\{M_1^{(0)}, M_2^{(0)}, M_3^{(0)}\} = \{0, M, -M\}$ corresponding to $\{N_1^{(0)}, N_2^{(0)}, N_3^{(0)}\} = \{(1,0,0)^T, (0,1,1)^T, (0,1,-1)^T\}$. This is obvious from the block diagonal structure of the matrix.

5.3.2 First-Order Corrections to the Eigenstates

The first-order corrections to the mass matrix's eigenstates can be computed via the standard non-degenerate perturbation theory procedure [74]. first-order corrections to eigenstates of an operator H with eigenvalues $\{\lambda_i^{(0)}\}$ from a perturbation ϵV are given by

$$|n\rangle^{(1)} = \frac{\langle k|\, V\, |n\rangle}{\lambda_n^{(0)} - \lambda_k^{(0)}} |k\rangle^{(0)} \tag{5.6}$$

Applying this equation to the mass matrix yields first-order states that can be written in the flavour basis as

$$N_1^{(0)} + \epsilon N_1^{(1)} = \left(1, -\tfrac{m_\tau}{M}, -\tfrac{m_\mu}{M}\right)^T \tag{5.7a}$$

$$N_2^{(0)} + \epsilon N_2^{(1)} = \frac{1}{\sqrt{2}}\left(\frac{m_\mu + m_\tau}{M},\ 1\ ,\ 1\right)^T \tag{5.7b}$$

$$N_3^{(0)} + \epsilon N_3^{(1)} = \frac{1}{\sqrt{2}}\left(\frac{m_\mu - m_\tau}{M},\ 1\ , -1\right)^T \tag{5.7c}$$

The first equation may initially seem surprising in that the N_τ content of the N_1 state is controlled by the coupling between N_e and N_μ, and vice-versa for the N_μ content. This is because the unperturbed matrix is a "flip" matrix that swaps N_μ and N_τ.

These states can be arranged in a matrix R. This is the matrix that maps the flavour basis to the mass basis for the right-handed neutrinos. Thus, this matrix is essential for our procedure of integrating out the two super heavy sterile states, while leaving the lightest sterile state as a propagating degree of freedom.

5.3.3 Second-Order Corrections to the Eigenvalues

The first-order mass corrections are given by the diagonal matrix elements of a perturbation. In our case the only diagonal perturbation is second-order and so we must calculate the additional contributions from the off-diagonal elements as they will also enter at second-order.

These small effects are important because they will determine the mass of the lightest eigenstate, N_1, to leading order. This is our dark matter candidate and we are principally interested in its phenomenology. The formula for calculating second-order corrections to eigenvalues in perturbation theory is given by

$$\lambda_n^{(2)} = \frac{|\langle k|\, V\, |n\rangle|^2}{\lambda_n^{(0)} - \lambda_k^{(0)}} \tag{5.8}$$

Applying this formula leads to

$$\epsilon^2 M_1^{(2)} = M_e + \frac{1}{2M}\left[\left(m_\mu^2 - m_\tau^2\right)^2 - \left(m_\mu + m_\tau\right)^2\right] \tag{5.9}$$

Since $m_\mu m_\tau / M \approx M_e$, we expect $M_1 \approx M_e$ if the hierarchy is satisfied because $M^{(2)}$ is the first non-vanishing correction to the lightest eigenstate's mass.

5.3.4 Integrating out the Super Massive Sterile States

In the ultraviolet our theory is defined by the Lagrangian density $\mathscr{L} = \mathscr{L}_N + \mathscr{L}_{other}$ where $\mathscr{L}_N$ contains all the terms that involve sterile states and $\mathscr{L}_{other}$ contains all of the other field content. After electro-weak and $U'(1)$

symmetry breaking, the sterile Lagrangian density is given by

$$\mathscr{L}_N \supset \bar{N}_i i\not{D} N_i - \frac{1}{2} M_{ij} N_i N_j + \langle h \rangle Y_{ij} N_i \nu_j \tag{5.10}$$

with $i \in \{e, \mu, \tau\}$ and where the both Y_{ij} and M_{ij} include any terms from the singlet scalar's vacuum expectation value. The scalar couplings have been excluded for brevity's sake (these can be easily recovered by tracking factors of m_μ and m_τ, as was done in Section 2.2.2). The multi-species covariant derivative is diagonal in this basis but that need not be true in the mass basis. To emphasize this point it is convenient to write

$$D^\mu_{ij} = \partial^\mu \mathbb{1}_{ij} - i g' Q_{ij} Z'^\mu \tag{5.11}$$

where the kinetic term is manifestly invariant under any set of unitary field redefinitions but the charge matrix Q_{ij} is basis dependent, because it is sensitive to any states containing N_μ or N_τ.

We wish to transform from the flavour basis, which is indexed by $i \in \{e, \mu, \tau\}$, to the mass basis, which is indexed by $a \in \{1, 2, 3\}$. To do this we must use the matrix R which is defined by $N_a = R_{ai} N_i$. To first-order R is determined by the perturbed eigenstates of the original mass matrix, and so R is given by

$$R = \begin{bmatrix} 1 & -\frac{m_\tau}{M} & -\frac{m_\mu}{M} \\ \frac{1}{\sqrt{2}} \frac{m_\mu + m_\tau}{M} & \frac{1}{\sqrt{2}} & \frac{1}{\sqrt{2}} \\ \frac{1}{\sqrt{2}} \frac{m_\mu - m_\tau}{M} & \frac{1}{\sqrt{2}} & -\frac{1}{\sqrt{2}} \end{bmatrix} \tag{5.12}$$

R is an orthogonal matrix and so we can insert $R^T R$ wherever we would like within the Lagrangian density. We may do so to eliminate all fields

N_i in favour of their mass basis counterparts N_a. If we wish to do this, we must make the following substitutions.

$$M_{ij} \to R_{ai} M_{ij} R^T_{jb} := \tilde{M}_{ab} \tag{5.13a}$$

$$Q_{ij} \to R_{ai} Q_{ij} R^T_{jb} := \tilde{Q}_{ab} \tag{5.13b}$$

$$Y_{ij} \to R_{ai} Y_{ij} := \tilde{Y}_{aj} \tag{5.13c}$$

We have now expressed the Lagrangian density in terms of N_1, N_2, and N_3 and integrated out N_2 and N_3. Our first step is to calculate the classical equations of motion in the zero momentum limit. The equations of motion in this limit are found by neglecting all derivative terms; this leads to

$$N_2 = -\frac{\langle h \rangle}{M_2} \tilde{Y}_{2j} \nu_j \tag{5.14a}$$

$$N_3 = -\frac{\langle h \rangle}{M_3} \tilde{Y}_{3j} \nu_j \tag{5.14b}$$

Setting the fields equal to these values, and only keeping operators of dimension-five or less, we arrive at the truncated effective Lagrangian density

$$\begin{aligned} \mathscr{L}_{IR} =& \bar{N}_1 (i\partial\!\!\!/ - M_1) N_1 + \langle h \rangle N_1 \tilde{Y}_{1j} \nu_j - \frac{\langle h \rangle^2}{2} \left(Y^T_{3\times 2} \tilde{M}^{-1}_{2\times 2} \tilde{Y}_{3\times 2} \right)_{ij} \nu_i \nu_j \\ &+ g' \bar{N}_1 \tilde{Q}_{11} Z' N_1 + g' \frac{\langle h \rangle}{M_2} \bar{N}_1 \tilde{Q}_{12} Z' \tilde{Y}_{2j} \nu_j + g' \frac{\langle h \rangle}{M_3} \bar{N}_1 \tilde{Q}_{13} Z' \tilde{Y}_{2j} \nu_j \end{aligned} \tag{5.15}$$

The dimension-five operators coming from the kinetic terms have been omitted because their contribution to any physical process will be suppressed by factors of $\left(\frac{y\langle h \rangle}{M}\right)^2$. The term in brackets has been written to emphasize that the left-handed neutrinos acquire a mass via the see-saw mechanism with a

2×3 Yukawa matrix and only two sterile states being integrated out. If we define $\nu_\Sigma := \frac{1}{\mathcal{N}} \tilde{Y}_{1j} \nu_j$, where

$$\mathcal{N} := \sqrt{\sum_i \tilde{Y}_{1i}^2} \tag{5.16}$$

then we have

$$\mathscr{L} \supset [\nu_\Sigma, N_1] \begin{bmatrix} m_\Sigma & \mathcal{N}\langle h \rangle \\ \mathcal{N}\langle h \rangle & M_1 \end{bmatrix} \begin{bmatrix} \nu_\Sigma \\ N_1 \end{bmatrix} \tag{5.17}$$

m_Σ is the Majorana mass of ν_Σ. In principle ν_Σ may not be a mass eigenstate. However, to a first approximation, the above expression should be valid and it is a convenient parametrization. Provided the Majorana mass terms for all of the Standard Model neutrinos are small compared to M_1, they have no effect on the mixing angle at leading order. There is no mixing between N_1 and the other active neutrino states that are orthogonal to ν_Σ. We see that, if we wish to diagonalize this mass matrix in the see-saw limit, the mixing angle is given by

$$\theta_m = \frac{\mathcal{N}\langle h \rangle}{M_1} \tag{5.18}$$

This analysis is easily generalized for non-zero mass-inducing operators. All that is required is to modify the unperturbed eigenstates of the mass matrix.

5.4 Mass-Inducing Operator Parametrics

In the previous chapter we found that, in the absence of Yukawa-inducing operators, one required non-vanishing mass-inducing operators to fit to

neutrino data. Although we only worked in the limit of $\delta M_\mu = 0$, the issues we encounter in this limit are exactly the same issue that are encountered for finite mass-inducing operators. Since this limit is simpler and equally illustrative we will restrict our discussion to this case exclusively.

Table 4.1 shows that all of the dimensionless parameters defined by Equation 4.5 required to fit the neutrino textures are within two orders of magnitude of unity. This condition is enough to obtain rough parametric dependence of various parameters to within two orders of magnitude. We can use this condition, and the hierarchy of sterile masses required for dark matter coupled with the relations in Equation 4.5, to see if galactic x-ray search bounds can be satisfied while simultaneously reproducing the correct neutrino phenomenology.

The hierarchy of $M >> m_\mu \approx m_\tau >> M_e$ and the condition of order one couplings implies a similar hierarchy for the Yukawa couplings in the theory. This is because

$$r := \sqrt{\frac{m_\tau y_\mu}{y_\tau m_\mu}} \approx \mathcal{O}(1) \tag{5.19a}$$

$$\mu := \frac{M}{\sqrt{m_\mu m_\tau}} \frac{y_e}{\sqrt{y_\mu y_\tau}} \approx \mathcal{O}(1) \tag{5.19b}$$

$$\mu_e := \frac{\sqrt{y_\mu y_\tau}}{y_e} \frac{M_e}{\sqrt{m_\mu m_\tau}} \approx \mathcal{O}(1) \tag{5.19c}$$

We see that the disparity in scales between the various masses must be accounted for by a disparity in size of the various Yukawa couplings to correctly account for neutrino phenomenology. This tells us that $\frac{y_e^2}{y_\mu y_\tau} \approx \mathcal{O}(\epsilon^2)$

and $y_\mu \approx y_\tau$. Lastly, we should consider the overall mass scale of the left-handed neutrino mass matrix. With the stated hierarchy of masses and Yukawa couplings, this is given parametrically by

$$\overline{\mathscr{M}} := \frac{\langle h \rangle^2}{\overline{m}_y} \frac{y_e^2 y_\mu y_\tau}{\mu\mu_e - 2}\mu \approx \langle h \rangle^2 \frac{y_e \sqrt{y_\mu y_\tau}}{\sqrt{m_\mu m_\tau}} \approx \frac{y_e^2 \langle h \rangle^2}{M_e} \tag{5.20}$$

where the final equality used the fact that $\frac{M_e}{\sqrt{m_\mu m_\tau}} \approx \frac{y_e}{\sqrt{y_\mu y_\tau}}$. Referring to Equation 5.3.3 and noting that $\frac{m_\mu m_\tau}{M} \approx M_e$ we see that $M_1 \approx M_e$; this has a physical interpretation as the mass of the dark matter candidate. Next we would like to connect y_e to some experimentally probed parameter. For a diagonal Yukawa matrix in the flavour basis the Yukawa matrix in the right-handed mass basis is given by

$$\tilde{Y} = \begin{bmatrix} y_e & -y_\mu \frac{m_\tau}{M} & -y_\tau \frac{m_\mu}{M} \\ \frac{1}{\sqrt{2}} \frac{m_\mu - m_\tau}{M} & \frac{1}{\sqrt{2}} & \frac{1}{\sqrt{2}} \\ \frac{1}{\sqrt{2}} \frac{m_\mu + m_\tau}{M} & \frac{-1}{\sqrt{2}} & \frac{1}{\sqrt{2}} \end{bmatrix} \tag{5.21}$$

This implies that $\mathscr{N} \approx y_e$. Noting that $\theta_m = \frac{\mathscr{N}\langle h \rangle}{M_1}$, we can re-express the overall mass scale as

$$\overline{\mathscr{M}} \approx M_1 \left(\frac{\mathscr{N}^2}{M_1^2} \right) = M_1 \theta_m^2 \approx M_e \sin^2 \theta_m \tag{5.22}$$

The sterile neutrino mass must be around $1 - 100$ keV to account for the dark matter energy density [7] and, for range of sterile dark matter masses, $\sin^2 \theta_m \leq 10^{-12}$; this leads to $\overline{\mathscr{M}} \approx 10^{-9} - 10^{-7}$eV. Neutrino oscillation data requires that the heaviest neutrino be at least $\sqrt{\Delta m_{13}^2} = 4.95 \cdot 10^{-2}$eV [8].

This massive disparity in scales is impossible to reconcile since the matrix is composed of order one numbers multiplied by the overall mass scale. The same parametric dependence is present with non-zero mass-inducing operators and so neutrino mass phenomenology is incompatible with the Z' progenitor scenario even with the inclusion of dimension-five mass-inducing operators.

5.5 Yukawa-Inducing Operator Parametrics

The Yukawa-inducing operators are not constrained by the same ordering as the mass-inducing operators. This is because the parametrics for the Lagrangian parameters are significantly different for the Yukawa-inducing operators when compared to the mass-inducing operators.

The relevant parameters are

$$X_\mu = \frac{Z_\mu}{y_\mu} \tag{5.23a}$$

$$X_\tau = \frac{Z_\tau}{y_\tau} \tag{5.23b}$$

$$\kappa_\mu = \frac{m_\mu}{\sqrt{M_e M}} \sqrt{\frac{y_\tau}{y_\mu}} \tag{5.23c}$$

$$\kappa_\tau = \frac{m_\tau}{\sqrt{M_e M}} \sqrt{\frac{y_\mu}{y_\tau}} \tag{5.23d}$$

$$\overline{\mathscr{M}}_Y = \frac{\langle h \rangle^2}{M} \frac{y_\mu y_\tau}{1 - 2\kappa_\mu \kappa_\tau} \tag{5.23e}$$

From the equations above we see that, provided $y_{\mu,\tau} \approx Z_{\mu,\tau}$ and $m_\mu \approx m_\tau$, we only require $m_{\mu,\tau} \approx \sqrt{MM_e}$ for all of the parameters that control mixing to be of order unity. This is required to fit to the neutrino texture data as shown in Table 4.2. This is easily achieved in conjunction with the sterile mass hierarchy required to provide a suitable dark matter candidate. The modified Yukawa coupling matrix written in the basis that diagonalizes the sterile mass matrix is given to first-order in perturbation theory by

$$\tilde{Y} = \begin{bmatrix} -\left(Z_\mu \frac{m_\tau}{M} + Z_\tau \frac{m_\mu}{M}\right) & -y_\mu \frac{m_\tau}{M} & -y_\tau \frac{m_\mu}{M} \\ \frac{1}{\sqrt{2}}\left(Z_\mu - Z_\tau\right) & \frac{1}{\sqrt{2}} & \frac{1}{\sqrt{2}} \\ \frac{1}{\sqrt{2}}\left(Z_\mu + Z_\tau\right) & \frac{-1}{\sqrt{2}} & \frac{1}{\sqrt{2}} \end{bmatrix} \tag{5.24}$$

If we assume an approximate $\mu \leftrightarrow \tau$ exchange symmetry we may speak loosely of $y \approx y_\mu \approx y_\tau$ and $Z \approx Z_\mu \approx Z_\tau$. Then $\mathcal{N} \approx y\frac{m}{M}$ (see Equation 5.3.4) since $Z \approx y$ by virtue of the fact that $X_{\mu,\tau} \approx \mathcal{O}(1)$ for all of the solutions presented in Table 4.2. Since the dark matter mass scale is fixed by M_e we can use the fact that $\kappa_{\mu,\tau} \approx \mathcal{O}(1)$ to see that when $M \to \alpha M$ $m \to \sqrt{\alpha} m$. Noting that left-handed mass scale is also bounded by neutrino texture data and cosmological considerations we can see that the Yukawa couplings also scale like $y \to \sqrt{\alpha} y$. The mixing angle is given by $\theta_m = \frac{\langle h \rangle \mathcal{N}}{M_1}$ and since the scaling of $\mathcal{N}$ goes like $\frac{ym}{M} \to \frac{ym}{M}\frac{\sqrt{\alpha}\sqrt{\alpha}}{\alpha}$ we see that the mixing angle is independent of our choice of M. One can solve for the mixing angle as

$$\sin^2\theta_m \approx \theta_m^2 = \left(\frac{\langle h \rangle \mathcal{N}}{M_1}\right)^2 \approx \frac{\langle h \rangle^2 y^2}{M}\frac{m^2}{MM_1}\frac{1}{M_1} \approx \frac{\overline{\mathcal{M}}_Y}{M_1} \tag{5.25}$$

With the final equality being given by the fact that $M_1 \approx m\frac{m}{M}$ (note this holds

even in the limit of $M_e = 0$). For $M_1 = 10\text{keV}$ and $\overline{\mathscr{M}}_Y = 0.01\text{eV}$ we arrive at $\sin^2\theta \approx 10^{-6}$ which violates the x-ray search bounds [75]. Thus we have shown that Yukawa-inducing operators, like the mass-inducing operators, cannot account for observed neutrino phenomenology in a manner which is consistent with the Z' progenitor scenario. Note that ta very similar relationship was found for the mass-inducing operators in the previous section.

5.6 Both Yukawa- and Mass-Inducing Operators

We have now shown that, for Yukawa and mass-inducing operators, our dark matter candidate cannot be involved in the production of neutrino masses. This is because if our dark matter candidate composes a significant fraction of the observed dark matter energy density then it's mixing with Standard Model states is severely constrained. This in turn constrains the ratio $m_{\mu,\tau}/M$. To conform to x-ray bounds one cannot obtain the correct neutrino textures in the simple models we considered

This analysis followed from considering Yukawa- and mass-inducing operators separately. There is the possibility that both types of operators are present. In this case we can examine in the limit where $m_\mu = m_\tau = 0$ to guarantee a totally decoupled $N_1 = N_e$ with y_e sufficiently small to satisfy

x-ray bounds and so that N_e does not significantly affect neutrino textures . Here we will have a 2x2 mass matrix and a 3x2 Yukawa matrix. This scenario can produce the correct neutrino, albeit with a plethora of coincidental ratios of scale.

This possible solution is paramount to considering the Z' progenitor and see-saw mechanisms are disjoint since the fields have been partitioned into two sets which are completely decoupled. One could argue it is equally well motivated to simply add a fourth sterile neutrino, which is uncharged under $U'(1)$, and decouple it from the other three. This would then represent the dark matter candidate and the neutrino textures would be controlled by the other three fields.

The left-handed mass matrix for a theory with non zero δM_μ,δM_τ,Z_μ, and Z_τ, but with vanishing y_e, m_μ , and m_τ is given by

$$M_L = \frac{y_\mu y_\tau \langle h \rangle^2}{M} \frac{1}{1-\kappa_\mu \kappa_\tau} \begin{bmatrix} -\kappa_\mu X_\tau^2 + 2X_\mu X_\tau - \kappa_\tau & \bullet & \bullet \\ X_\tau - \kappa_\tau X_\mu & -\kappa_\tau & \bullet \\ X_\mu - \kappa_\mu X_\tau & 1 & -\kappa_\mu \end{bmatrix} \tag{5.26}$$

with the following definitions:

$$X_\mu = \frac{Z_\mu}{y_\mu} \tag{5.27a}$$

$$X_\tau = \frac{Z_\tau}{y_\tau} \tag{5.27b}$$

$$\kappa_\mu = \frac{\delta M_\mu}{M} \frac{y_\tau}{y_\mu} \tag{5.27c}$$

Hierarchy	$\frac{m_\ell}{m_2}$	X_μ	X_τ	κ_μ	κ_τ	$\sqrt{\kappa_\mu \kappa_\tau}$
Normal	0	0.595027	−0.338739	0.85531	0.7059	0.7770
Normal	0	0.595027	−0.338739	1.41738	1.16849	1.2869
Inverted	0	−4.50355	−4.95879	0.95494	1.14328	1.0448
Inverted	0	−4.50355	−4.95879	1.44039	0.370025	0.7301

Table 5.1: Parameter values for Yukawa-inducing operators and mass-inducing operators in a $y_e = 0$, $m_\mu = m_\tau = 0$ limit that fit to the data. $\frac{m_\ell}{m_2}$ is the ratio of the lightest mass to m_2.

$$\kappa_\tau = \frac{\delta M_\tau}{M} \frac{y_\mu}{y_\tau} \tag{5.27d}$$

This very similar structurally to the case of the Yukawa-inducing operators with non vanishing m_μ and m_τ and as a result the solutions for both actually have identical X_μ and X_τ however due to the slight difference in the κ parameter definitions these take on different values. The results are summarized in Table 5.1. The parameters κ_μ and κ_τ are required to be $\mathcal{O}(1)$ to explain the observed neutrino textures. The quantity $\sqrt{\kappa_\mu \kappa_\tau} = \frac{\sqrt{\delta M_\mu \delta M_\tau}}{M}$ is a useful measure of the relative sizes of the mass terms induced by the dimension-five operators because it is independent of the Yukawa couplings.

The δM_μ terms arise from operators of the form $\delta_\mu \frac{1}{\Lambda} S S L_e \tilde{H} N_\mu$ and so $\delta M_\mu = \delta_\mu \langle S \rangle \frac{\langle S \rangle}{\Lambda}$ (the same story holds for δM_τ). Provided $\frac{M}{\delta_{\mu,\tau} \langle S \rangle} \approx \frac{\langle S \rangle}{\Lambda}$, the

approximate equivalence of $\delta M_{\mu,\tau}$ and M is consistent within the framework of effective field theory.

If we include both mass- and Yukawa-inducing dimension-five operators the correct neutrino phenomenology can be generated even in the limit of a totally decoupled N_e. This leaves N_e to lend itself as a dark matter candidate for the model.

It should be noted that for the inclusion of only mass- and Yukawa-inducing operators the neutrino masses must be generated by only two of the right-handed states. This leads to a massless lightest neutrino, however we have neglected the aforementioned Weinberg-inducing operators that could have supplied mass terms to the left-handed mass matrix directly. This could accommodate three massive right-handed neutrinos.

CHAPTER 6

CONCLUSIONS AND FUTURE DIRECTIONS

In this thesis we were interested in determining if the progenitor scenario described by Shuve and Yavin could manifest itself in a model which simultaneously explained the observed neutrino textures. We found that a model with three right-handed neutrinos labelled by the same generational indices as the Standard Model leptons was not capable of reproducing observed neutrino textures.

However this highly minimalistic model was able to capture the qualitative features of the observed neutrino textures quite well and was also able to achieve quantitative agreement within about 25%. The model naturally gives a near maximal θ_{23} and is capable of fitting on of the two angles θ_{12}

or θ_{13}. This is perhaps suggestive that lepton flavour symmetries may play a role in the structure of neutrino masses.

Subsequently, modifications with dimension five operators were investigated and it was found that these extended models could reproduce the observed neutrino textures for multiple sets of Lagrangian parameters. The magnitude of these dimension five operators in comparison to the dimension four operators were found to be self consistently small as would be suggested by an effective field theory picture. These operators came in two distinct sub-classes mass- and Yukawa-inducing operators. Both were capable of reproducing the neutrino phenomenology.

The Yukawa- type operators' dimensionless scaling parameters Z_μ and Z_τ were found to be on the same order as Yukawa couplings y_μ and y_τ. This is entirely consistent with the description as an effective field theory because the Yukawa couplings were found to be on the order of 10^{-6} for dark matter masses on the order of 10 keV. Thus one could imagine an ultraviolet completion in which the parameters that are associated with these dimension five operators are on the order of say 10^{-2} at high energies, but, due to suppression from energy scale ratios in the infrared, these parameters are on the order of the Yukawa couplings y_μ and y_τ at lower energies.

The mass-inducing operators were found to be on the order of the other

masses in the theory and similarly could be imagined to arise from a stronger coupling in the ultraviolet that is suppressed by ratios of the infrared energy scale to the cutoff energy scale. The naive expectation is that the mass terms generated by these operators go something like $g\langle S\rangle(g\langle S\rangle/\Lambda)$. Therefore provided $\Lambda > g\langle S\rangle > m_{\mu,\tau}$ the equivalence of the mass terms coming from dimension-five operators and dimension-four operators is easily accommodated.

The fact that the neutrino textures require additional dimension five operators suggests that this minimalist approach must be relaxed. These operators can be generated via additional right-handed states. The mass of these states would play the role of Λ and one could imagine integrating them out to obtain the effective theory we considered in this thesis.

The parametrics required to fit the neutrino textures in our model suggest an unacceptably large amount of mixing with the Standard Model leptons if one wishes to identify the lightest sterile as a dark matter candidate and to employ the Shuve-Yavin Z' production mechanism. This was found to be a generic feature that could not be avoided without decoupling the fields responsible for the see-saw mechanism and the dark matter candidate. The tension was that a sterile neutrino's (in this case the dark matter candidate's) contribution to the active neutrino mass matrix is parametrically

given by

$$\frac{y_{DM}^2 \langle h \rangle^2}{m_{DM}} = m_{DM}\theta_m^2 \tag{6.1}$$

where m_{DM} is the mass of the dark matter candidate and y_{DM} is it's only Yukawa coupling to some linear combination of Standard Model neutrinos. The equality in Equation 6 made use of the see-saw mixing angle formula $\theta_m = \frac{y_{DM}\langle h \rangle}{m_{DM}}$. As an example the bounds on 10 keV sterile neutrino dark matter set $\theta_m^2 < 10^{-12}$ [11, 58] leading to a contribution to the active neutrino masses on the order of 10^{-8} eV: approximately six orders of magnitude below the minimum characteristic mass scale for the heaviest neutrino.

This tells us that even if we were to expand the matter content sufficiently to allow for a dark matter candidate it would not contribute significantly to neutrino mass generation. This argument is general and will be a generic consequence of models with sterile neutrinos as a dark matter candidate.

Although the dark matter candidate's coupling to the Standard Model is sufficiently restricted that it cannot contribute significantly to the production of neutrino masses, the Z' progenitor scenario and neutrino oscillation data are not in conflict with one another. They may be accommodated within a single model however the degrees of freedom required to realize one mechanism are independent of the degrees of freedom to fit the other.

This is an important lesson about sterile neutrino dark matter because it tells us that it is in some sense less well motivated than one would naively

expect. At least the observation of neutrino masses does not imply a well motivated dark matter candidate in our model as it would necessarily not be involved in the production of the observed neutrino masses. This feature is one which we would generally expect to see in other models of sterile neutrinos.

The Z' progenitor model remains a viable possibility to explain the observed dark matter abundance for sterile neutrino dominated dark matter. The dark matter candidate in these types of models does not seem to be capable of contributing significantly to active neutrino's mass structure and it's contributions should be considered a sub dominant effect. Additionally we found that the charge structure implied by local $L_\mu - L_\tau$ symmetry that is spontaneously broken seems to naturally generate neutrino textures that are similar to those that are observed.

The analysis at the end of Chapter 5 showed that, provided a coincidence in the ratio of scales occurred, with both Yukawa- and mass-inducing operators N_μ and N_τ can generate the neutrino textures while N_e acts as a dark matter candidate.

This possibility is also easily realized in the context of a gauged $B-L$ because there are no restrictions on the form of the right-handed mass matrix or on the Yukawa coupling matrix. The right-handed mass terms would be generated via a single order parameter in the same way as in our theory and

this breaking pattern would populate every entry in the mass matrix. No dimension five operators would be needed. The unattractive feature of this proposal compared to that involving a lepton flavour symmetry is that the model provides no explanation for the structure of the neutrino textures and a large number of parameters must be set to zero due to phenomenological considerations with no theoretical motivation.

Never the less it may be worth investigating the parametrics of the Shuve Yavin progenitor scenario in the case of $B-L$. Bounds on $B-L$ would have to be investigated to see if the parametrically viable region for the progenitor scenario is still viable, and to determine if this possibility is self consistent and if the hypothesis could be tested or constrained by any current experiments.

APPENDIX A

A Brief Review of the Higgs Mechanism in the Context of the Standard Model

The Standard Model incorporates a number of non-trivial features of quantum field theory. It contains spontaneous breaking, CP violation, non-Abelian gauge symmetries, and accidental symmetries; I will give a brief review of its features. The Standard Model is defined by the gauge group $SU(3)\otimes SU(2)\otimes U(1)$ and its matter content which transforms in the representations shown in Table A [13]. The Standard Model doublet fields are defined as

$$L_e = \begin{pmatrix} \nu_e \\ e \end{pmatrix} \tag{A.1a}$$

$$Q_u = \begin{pmatrix} u \\ d \end{pmatrix} \tag{A.1b}$$

$$H = \begin{pmatrix} \phi^+ \\ \phi^0 \end{pmatrix} \tag{A.1c}$$

$$\tilde{H} = \epsilon H^* = \begin{pmatrix} \phi^{0*} \\ -\phi^{+*} \end{pmatrix} \tag{A.1d}$$

Where e is the left handed component of the electron field, ν_e is the left handed electron neutrino and u and d are the left handed up and down quarks respectively; all fields are two component Weyl spinors (for a good review of two component spinor techniques see [76]). H is the Higgs doublet. Note that H and $\tilde{H}$ transform identically under $SU_L(2)$ but have opposite hypercharge Y. This is what allows for the generation of mass terms for both the up and down quark with a single Higgs field. One may then employ the definitions above and write down every possible renormalizable interaction possible to obtain the Standard Model Lagrangian. The explicit form of this Lagrangian including field strength tensors, covariant derivatives, and Yukawa interactions is very lengthy and is nicely summarized in Chapter Two of The Standard Model A Primer by Burgess and Moore [13] (in this text four component Dirac spinors are used instead of two component Weyl spinors). The important feature for our analysis is how particles go about acquiring a mass.

In the Standard Model to maintain gauge invariance the masses are gener-

Field	$U_Y(1)$	$SU_L(2)$	$SU_c(3)$
L_m	$-\frac{1}{2}$	2	$\mathbb{1}$
Q_n	$+\frac{1}{6}$	2	3
e^c_m	1	$\mathbb{1}$	1
u^c_n	$-\frac{2}{3}$	$\mathbb{1}$	$\overline{3}$
d^c_n	$+\frac{1}{3}$	$\mathbb{1}$	$\overline{3}$
H	$-\frac{1}{2}$	2	$\mathbb{1}$
$\tilde{H}$	$+\frac{1}{2}$	2	$\mathbb{1}$

Table A.1: Charge assignments of the fermionic and scalar fields in the Standard Model. The gauge bosons transform in the adjoint representation. The indices $m \in \{e, \mu, \tau\}$ and $n \in \{u, c, t\}$ denote the generations of leptons or quarks respectively (i.e. $d_c := s$ the strange quark). All fermionic fields are defined as left-handed Weyl spinors. The triplet representations under $SU_c(3)$ are indexed by colour while the first generation $SU_L(2)$ are defined in Equation A.1 the additional generations are obtained by trivial substitution. The nomenclature for groups is such that the number is the dimension of the representation while the bar differentiates between objects transforming as a tensor with upper indices (bar) v.s. with lower indices (no bar) (see Coleman Aspects of Symmetry [9])

ated by the spontaneous breaking of the Higgs doublet. This is achieved via the potential

$$V\left(H^{\dagger}H\right)=\frac{\lambda}{4}\left(H^{\dagger}H-\frac{\langle h\rangle^{2}}{2}\right)^{2} \tag{A.2}$$

This is minimized by the solution $H^{\dagger}H=\frac{1}{2}\langle h\rangle^{2}$ and with no loss of generality we can choose our basis such that this vacuum expectation value points along the real component of ϕ^{0}. Thus for the purposes of mass generation we may make the substitution

$$H\rightarrow\frac{1}{\sqrt{2}}\begin{pmatrix}0\\ \langle h\rangle\end{pmatrix} \tag{A.3}$$

Then combinations which are allowed by gauge invariance which initially have the form of Yukawa couplings take on the form of masses for various particles. For example the combination

$$\mathscr{L}\supset y_{e}L_{e}He^{c}\rightarrow\frac{1}{\sqrt{2}}y_{e}\langle h\rangle ee^{c}:=m_{e}ee^{c} \tag{A.4}$$

where we have defined the quantity $m_{e}:=\frac{1}{\sqrt{2}}y_{e}\langle h\rangle$ and this is the Dirac mass of the electron. If one only considers one generation the up and down quark masses are generated by the operators $\tilde{y}_{u}Q_{u}\tilde{H}u^{c}$ and $y_{d}Q_{u}Hd^{c}$ respectively. Neutrinos are massless in the Standard Model because the matter content does not provide a fermionic field that would allow for the generation of a neutrino mass via the Higgs mechanism in a renormalizable theory. This is because $L\tilde{H}$ is a singlet under the Standard Model gauge group, but not under Lorentz transformations. To achieve Lorentz invariance we would need a two component spinor that is uncharged under the Standard Model.

When additional generations are included the Yukawa couplings are promoted to matrices and the couplings have the form $\tilde{y}_{nn'}Q_n\tilde{H}u^c_{n'}$ and $y_{nn'}Q_nHd^c_{n'}$. This couples the right handed quarks of one generation to the left handed quarks of another.

Some selected original literature on the subject of the Standard Model's development include the following [59, 77–79].

APPENDIX B

METHOD FOR EXTRACTING LAGRANGIAN PARAMETERS

To determine if the theories we considered in this thesis could reproduce neutrino masses we generated all possible matrices that could produce the correct neutrino phenomenology in the *CP* conserving limit and then expressed these matrices in the flavour basis. In this appendix I will review the basic methodology.

The goal was to be able to extract combinations of Lagrangian parameters which would fit the neutrino data from nu-Fit [8] exactly. As a result all of the mixing parameters employed can be found on nu-Fit's website which provides a global fit of the neutrino mixing parameters.

B.1 Generating the Correct Mass Spectra

The measurements of Δm^2_{12} and Δm^2_{13} allow the set of three neutrino masses $\{m_1, m_2, m_3\}$ to be parametrized by only one variable. If one specifies the value of m_2, and the hierarchy, the absolute values of $m_1$and m_3 are known. Eigenstates $\{\nu_1, \nu_2, \nu_3\}$ are defined by their composition in the flavour basis (i.e. ν_1 is the "mostly ν_e" state).

The key observation is that

$$\frac{\Delta m^2_{13}}{\Delta m^2_{12}} = 32.76 \qquad \text{(NH)} \tag{B.1a}$$

$$\frac{\Delta m^2_{23}}{\Delta m^2_{12}} = 32.65 \qquad \text{(IH)} \tag{B.1b}$$

For the Normal Hierarchy this allows us to define the heaviest neutrino mass in terms of m_2 and the lightest neutrino mass.

$$|m_3| = \sqrt{32.76\left(m_2^2 - m_1^2\right) + m_1^2} \qquad \text{(NH)} \tag{B.2a}$$

$$|m_1| = \sqrt{m_2^2 - \frac{(m_2^2 - m_3^2)}{32.65}} \qquad \text{(IH)} \tag{B.2b}$$

There is no positivity condition on the eigenvalues of a fermionic mass matrix and as a result the relative signs of the neutrino masses is undetermined. We consider separately to four different possibly sign combinations $\{+,+.+\}$, $\{-,+.+\}$,$\{+,-.+\}$, $\{+,+.-\}$ corresponding to the sign of $\{m_1, m_2, m_3\}$. This accounts for all possible sign choices because all other possibilities can be obtained via a multiplication by $-\mathbb{1}$.

For the rest of this discussion we will restrict ourselves to the case of the Normal Hierarchy to avoid redundancy. At this point we have just generated the diagonal left handed neutrino matrix in the mass basis written

$$M_L = \begin{bmatrix} m_1 & 0 & 0 \\ 0 & m_2 & 0 \\ 0 & 0 & m_3(m_1, m_2) \end{bmatrix} \tag{B.3}$$

B.2 Re-expressing in the Flavour Basis

This matrix can then be "rotated" into the flavour basis by multiplying by the PMNS matrix on the right and its inverse on the left. To do this we must first construct the PMNS matrix from the mixing data.

This is done via the standard parametrization of the PMNS matrix given below with c_{ij} (s_{ij}) being shorthand for $\cos\theta_{ij}(\sin\theta_{ij})$.

$$\begin{bmatrix} \nu_e \\ \nu_\mu \\ \nu_\tau \end{bmatrix} = \begin{bmatrix} c_{13}c_{12} & -c_{13}s_{12} & s_{13}e^{-i\delta} \\ -s_{23}s_{13}c_{12}e^{i\delta} - c_{23}s_{12} & -s_{23}s_{13}s_{12}e^{i\delta} + c_{23}c_{12} & s_{23}c_{13} \\ -c_{23}s_{13}c_{12}e^{i\delta} + s_{23}s_{12} & -c_{23}s_{13}s_{12}e^{i\delta} - s_{23}c_{12} & c_{23}c_{13} \end{bmatrix} \begin{bmatrix} \nu_1 \\ \nu_2 \\ \nu_3 \end{bmatrix} \tag{B.4}$$

For our purposes $\delta = 0$ because we are working within the CP conserving limit. It is simply a matter of using the mixing angle data from [8] to reconstruct this matrix. It is important to use the correct value of θ_{23} because it is different depending on the hierarchy of interest.

After multiplying on the left and right of the mass matrix we have a new mass matrix written in the flavour basis let us denote this M_L' or written

explicitly

$$M_L' = PMNS^T \cdot M_L \cdot PMNS \tag{B.5}$$

B.3 Strategy to find Candidates for our Theory

For the subsequent discussion let us restrict ourselves to the model as it is presented in Chapter 2 (i.e. no dimension-five operators). The left handed mass matrix in that particular scenario was parametrized by the set of parameters $\{r, \mu, \mu_e, \overline{\mathscr{M}}\}$ and could be written

$$M_L' = \overline{\mathscr{M}} \begin{bmatrix} 1 & -\frac{r}{\mu} & -\frac{r^{-1}}{\mu} \\ -\frac{r}{\mu} & \frac{r^2}{\mu^2} & \frac{\mu\cdot\mu_e - 1}{\mu^2} \\ -\frac{r^{-1}}{\mu} & \frac{\mu\cdot\mu_e - 1}{\mu^2} & \frac{r^{-2}}{\mu^2} \end{bmatrix} \tag{B.6}$$

So if we define $\Omega := \frac{1}{M_{11}'} M_L'$, where the L subscript has been omitted in the denominator in the interest of indices, then we see that our theory predicts all M_L' to have the property that $\Omega_{12}^2 = \Omega_{22}$ and $\Omega_{13}^2 = \Omega_{33}$. If we define

$$r_{ii} := \frac{\Omega_{1i}^2}{\Omega_{ii}} \tag{B.7}$$

So if we find a mass matrix that does not satisfy the condition $r_{11} = r_{22} = 1$ then our theory is incapable of producing it. So if we take all of the M_L' generated from the nu-Fit neutrino data, and normalize them by their entry in the first row and first column, we can check to see if any of them satisfy

this criteria. To do this we can plot r_{11} and r_{22} as a function of m_1 in the interval $m_1 \in [0, m_2]$ and look for some point where $r_{11} = r_{22} = 1$ if no such point exists for all of the possible sign combinations, and this is true for both hierarchies, then our theory cannot reproduce the global fit values.

B.4 Extracting Lagrangian Parameters

If a fit is found (as was the case when dimension-five operators were included) then to extract the Lagrangian parameters is a simple exercise in algebra. Let us examine the case of the mass type operators. There the mass matrix was given by

$$M_L = \overline{\mathscr{M}} \begin{bmatrix} 1 & -\frac{r}{\mu} & -\frac{r^{-1}}{\mu} + \delta_\mu \frac{r}{\mu} \\ -\frac{r}{\mu} & \frac{r^2}{\mu^2} & \frac{\mu \cdot \mu_e - 1}{\mu^2} \\ -\frac{r^{-1}}{\mu} + \delta_\mu \frac{r}{\mu} & \frac{\mu \cdot \mu_e - 1}{\mu^2} & \frac{r^{-2}}{\mu^2} - \delta_\mu \frac{\mu_e}{\mu} \end{bmatrix} \tag{B.8}$$

From this one can equate the bracketed portion of the matrix with the Ω that has been generated from nu-Fit oscillation data. Here the condition from the previous section is relaxed to $r_{22} = 1$ and so only matrices which satisfied this criteria were kept. After some algebra one has

$$r^{-1} = \sqrt{\frac{\Omega_{33} - \frac{\Omega_{13}\Omega_{23}}{\Omega_1 2}}{\Omega_{12}\Omega_{13} - \Omega_{23}}} \tag{B.9a}$$

$$\mu = -\frac{r}{\Omega_{12}} \tag{B.9b}$$

$$\mu_e = \mu \left(\Omega_{23} + \Omega_{12}^{-2} r^{-2} \right) \tag{B.9c}$$

$$\delta_\mu = r^{-2} - \frac{\Omega_{13}}{\Omega_{12}} \tag{B.9d}$$

This gives the necessary parameters to reproduce the central values of the nu-Fit global neutrino mixing data. Perturbation theory can be used to study small departures from these solutions.

BIBLIOGRAPHY

[1] K.A. Olive et al.

Review of Particle Physics.

Chin.Phys., C38:090001, 2014.

[2] Y. Fukuda et al.

Evidence for oscillation of atmospheric neutrinos.

Phys.Rev.Lett., 81:1562–1567, 1998.

[3] Q.R. Ahmad et al.

Direct evidence for neutrino flavor transformation from neutral current interactions in the Sudbury Neutrino Observatory.

89:011301, 2002.

[4] G.W. Bennett et al.

Final Report of the Muon E821 Anomalous Magnetic Moment Measurement at BNL.

Phys.Rev., D73:072003, 2006.

[5] Kaoru Hagiwara, Ruofan Liao, Alan D. Martin, Daisuke Nomura, and Thomas Teubner.
$(g-2)_m u$ and alpha(M_Z^2) re-evaluated using new precise data.
J.Phys., G38:085003, 2011.

[6] A.D. Dolgov.
Neutrinos in cosmology.
Nucl.Phys.Proc.Suppl., 48:5–12, 1996.

[7] Brian Shuve and Itay Yavin.
Dark matter progenitor: Light vector boson decay into sterile neutrinos.
Phys.Rev., D89(11):113004, 2014.

[8] M.C. Gonzalez-Garcia, Michele Maltoni, and Thomas Schwetz.
Updated fit to three neutrino mixing: status of leptonic CP violation.
JHEP, 1411:052, 2014.

[9] Sidney Coleman.
Aspects of Symmetry.
Cambridge University Press, 1985.

[10] Dan Hooper.
TASI 2008 Lectures on Dark Matter.
pages 709–764, 2009.

[11] Alexey Boyarsky, Jukka Nevalainen, and Oleg Ruchayskiy.

Constraints on the parameters of radiatively decaying dark matter from the dark matter halo of the Milky Way and Ursa Minor.
Astron.Astrophys., 471:51–57, 2007.

[12] M. Williams, C.P. Burgess, Anshuman Maharana, and F. Quevedo.
New Constraints (and Motivations) for Abelian Gauge Bosons in the MeV-TeV Mass Range.
JHEP, 1108:106, 2011.

[13] Cliff Burgess and Guy Moore.
The Standard Model: A Primer.
Cambridge University Press, Cambridge, USA, 2007.

[14] P.A.R. Ade et al.
Planck 2013 results. XVI. Cosmological parameters.
Astron.Astrophys., 571:A16, 2014.

[15] C.P. Burgess.
An Ode to effective Lagrangians.
1998.

[16] Kenneth G. Wilson and Michael E. Fisher.
Critical exponents in 3.99 dimensions.
Phys.Rev.Lett., 28:240–243, 1972.

[17] Kenneth G. Wilson.

Renormalization group and critical phenomena. 1. Renormalization group and the Kadanoff scaling picture.

Phys.Rev., B4:3174–3183, 1971.

[18] Joseph Polchinski.

Effective field theory and the Fermi surface.

1992.

[19] Anthony Zee.

Quantum Field Theory in a Nutshell.

Cambridge University Press, Cambridge, USA, 2003.

[20] Steven Weinberg.

Quantum Theory of Fields.

Cambridge University Press, Cambridge, USA, 1995.

[21] Steven Weinberg.

Baryon and Lepton Nonconserving Processes.

Phys.Rev.Lett., 43:1566–1570, 1979.

[22] E. Noether.

Invariante Variationsprobleme.

Nachr. v. d. Ges. d. Wiss. zu Gottingen, pages 235–257, 1918.

[23] Stephen L. Adler.

Axial vector vertex in spinor electrodynamics.

Phys.Rev., 177:2426–2438, 1969.

[24] J.S. Bell and R. Jackiw.

A pcac puzzle: neutral pion decaying to two photons in the sigma-model.

Il Nuovo Cimento A, 60(1):47–61, 1969.

[25] Mark Srednicki.

Quantum Field Theory.

Cambridge University Press, Cambridge, USA, 2007.

[26] Peskin and Schroeder.

Introduction to Quantum Field Theory.

Westview Press, Boulder,USA, 1995.

[27] Xiao-Gang He, Girish C. Joshi, H. Lew, and R.R. Volkas.

Simplest Z-prime model.

Phys.Rev., D44:2118–2132, 1991.

[28] Nicola Cabibbo.

Unitary Symmetry and Leptonic Decays.

Phys.Rev.Lett., 10:531–533, 1963.

[29] Makoto Kobayashi and Toshihide Maskawa.

CP Violation in the Renormalizable Theory of Weak Interaction.

Prog.Theor.Phys., 49:652–657, 1973.

[30] S.M. Bilenky and Carlo Giunti.

Neutrinoless double-beta decay: A brief review.

Mod.Phys.Lett., A27:1230015, 2012.

[31] B. Pontecorvo.

Neutrino Experiments and the Problem of Conservation of Leptonic Charge.

Sov.Phys.JETP, 26:984–988, 1968.

[32] Andre de Gouvea, Alexander Friedland, and Hitoshi Murayama.

The Dark side of the solar neutrino parameter space.

Phys.Lett., B490:125–130, 2000.

[33] Zwicky.

Die Rotverschiebung von extragalaktischen Nebeln.

Helvetica Physica Acta., 6:110–127, 1933.

[34] Vera C. Rubin and Jr. Ford, W. Kent.

Rotation of the Andromeda Nebula from a Spectroscopic Survey of Emission Regions.

Astrophys.J., 159:379–403, 1970.

[35] M. S. Roberts.

The Rotation Curve of Galaxies.

In A. Hayli, editor, *Dynamics of the Solar Systems*, volume 69 of *IAU Symposium*, page 331, 1975.

[36] V. C. Rubin, W. K. J. Ford, and N. . Thonnard.

Rotational properties of 21 SC galaxies with a large range of luminosities and radii, from NGC 4605 /R = 4kpc/ to UGC 2885 /R = 122 kpc/.

Astrophys.J., 238:471–487, June 1980.

[37] Massimo Persic, Paolo Salucci, and Fulvio Stel.

The Universal rotation curve of spiral galaxies: 1. The Dark matter connection.

Mon.Not.Roy.Astron.Soc., 281:27, 1996.

[38] Y. Sofue and V. Rubin.

Rotation Curves of Spiral Galaxies.

Annual Review of Astronomy and Astrophysics, 39:137–174, 2001.

[39] A.N. Taylor, S. Dye, Thomas J. Broadhurst, N. Benitez, and E. van Kampen.

Gravitational lens magnification and the mass of abell 1689.

Astrophys.J., 501:539, 1998.

[40] Marusa Bradac, Douglas Clowe, Anthony H. Gonzalez, Phil Marshall, William Forman, et al.

Strong and weak lensing united. 3. Measuring the mass distribution of the merging galaxy cluster 1E0657-56.

Astrophys.J., 652:937–947, 2006.

[41] Maxim Markevitch, A.H. Gonzalez, D. Clowe, A. Vikhlinin, L. David, et al.

Direct constraints on the dark matter self-interaction cross-section from the merging galaxy cluster 1E0657-56.

Astrophys.J., 606:819–824, 2004.

[42] CDMS II Collaboration et. al.

Dark Matter Search Results from the CDMS II Experiment.

Science, 327:1619–, March 2010.

[43] C. E. et. al. Aalseth.

CoGeNT: A search for low-mass dark matter using p-type point contact germanium detectors.

Physical Review D., 88(1):012002, July 2013.

[44] V. Gehman.

Direct Search for Dark Matter with Two-Phase XENON Detectors: Current Status of Lux and Plans for LZ.

Frascati Phys.Ser., 58:51, 2014.

[45] K. Rielage et al.

Update on the MiniCLEAN Dark Matter Experiment.

Phys.Procedia, 61:144–152, 2015.

[46] J.J. Walding.

The DEAP Search For Dark Matter.

pages 193–196, 2014.

[47] T. Saab.

An Introduction to Dark Matter Direct Detection Searches and Techniques.

In K. Matchev and et al., editors, *The Dark Secrets of the Terascale (TASI 2011) - Proceedings of the 2011 Theoretical Advanced Study Institute in Elementary Particle Physics. Edited by Matchev Konstantin et al. Published by World Scientific Publishing Co. Pte. Ltd., 2013. ISBN #9789814390163, pp. 711-738*, pages 711–738, December 2013.

[48] Lars Bergstrom, Piero Ullio, and James H. Buckley.

Observability of gamma-rays from dark matter neutralino annihilations in the Milky Way halo.

Astropart.Phys., 9:137–162, 1998.

[49] Esra Bulbul, Maxim Markevitch, Adam Foster, Randall K. Smith, Michael Loewenstein, et al.

Detection of An Unidentified Emission Line in the Stacked X-ray spectrum of Galaxy Clusters.

Astrophys.J., 789:13, 2014.

[50] E. Kolb and M. Turner.

The Early Universe.

Frontiers in physics. Westview Press, 1994.

[51] Howard Baer, Ki-Young Choi, Jihn E. Kim, and Leszek Roszkowski.
Dark matter production in the early Universe: beyond the thermal WIMP paradigm.
Phys.Rept., 555:1–60, 2014.

[52] Joel R. Primack.
Dark matter and structure formation.
1997.

[53] A. Bastidas Fry, F. Governato, A. Pontzen, T. Quinn, M. Tremmel, et al.
All about baryons: revisiting SIDM predictions at small halo masses.
2015.

[54] Scott Dodelson and Lawrence M. Widrow.
Sterile-neutrinos as dark matter.
Phys.Rev.Lett., 72:17–20, 1994.

[55] Julien Lesgourgues and Sergio Pastor.
Neutrino cosmology and Planck.
New J.Phys., 16:065002, 2014.

[56] Dirk Notzold and Georg Raffelt.
Neutrino Dispersion at Finite Temperature and Density.
Nucl.Phys., B307:924, 1988.

[57] Jun Wu, Chiu Man Ho, and Daniel Boyanovsky.

Sterile neutrinos produced near the electroweak scale: Mixing angles, msw resonances, and production rates.

Phys. Rev. D, 80:103511, Nov 2009.

[58] Alexander Kusenko.

Sterile neutrinos: The Dark side of the light fermions.

Phys.Rept., 481:1–28, 2009.

[59] Peter W. Higgs.

Broken Symmetries and the Masses of Gauge Bosons.

Phys.Rev.Lett., 13:508–509, 1964.

[60] Mathew D. Schwartz.

Quantum Field Theory of Fields.

Cambridge University Press, Cambridge, USA, 2014.

[61] D. Cohen.

Lecture Notes in Statistical Mechanics and Mesoscopics.

ArXiv e-prints, July 2011.

[62] A. Abulencia et al.

Search for high-mass resonances decaying to e mu in $p\bar{p}$ collisions at $\sqrt{s}$ = 1.96-TeV.

Phys.Rev.Lett., 96:211802, 2006.

[63] J. Alcaraz et al.

A Combination of preliminary electroweak measurements and constraints on the standard model.

2006.

[64] T. Aaltonen et al.

Search for new physics in high mass electron-positron events in $p\bar{p}$ collisions at $\sqrt{s}$ = 1.96-TeV.

Phys.Rev.Lett., 99:171802, 2007.

[65] Ennio Salvioni, Alessandro Strumia, Giovanni Villadoro, and Fabio Zwirner.

Non-universal minimal Z' models: present bounds and early LHC reach.

JHEP, 1003:010, 2010.

[66] Wolfgang Altmannshofer, Stefania Gori, Maxim Pospelov, and Itay Yavin.

Neutrino Trident Production: A Powerful Probe of New Physics with Neutrino Beams.

Phys.Rev.Lett., 113:091801, 2014.

[67] Seungwon Baek, N.G. Deshpande, X.G. He, and P. Ko.

Muon anomalous g-2 and gauged L(muon) - L(tau) models.

Phys.Rev., D64:055006, 2001.

[68] R. Wendell et al.

Atmospheric neutrino oscillation analysis with sub-leading effects in Super-Kamiokande I, II, and III.

Phys.Rev., D81:092004, 2010.

[69] K. Abe et al.

Solar neutrino results in Super-Kamiokande-III.

Phys.Rev., D83:052010, 2011.

[70] B. Aharmim et al.

Measurement of the ν_e and Total ^{8}B Solar Neutrino Fluxes with the Sudbury Neutrino Observatory Phase-III Data Set.

Phys.Rev., C87(1):015502, 2013.

[71] Bei-Zhen Hu.

Recent Results from Daya Bay Reactor Neutrino Experiment.

2015.

[72] J. J. Gomez-Cadenas and Justo Martin-Albo.

Phenomenology of neutrinoless double beta decay.

PoS, GSSI14:004, 2015.

[73] J. Schechter and J. W. F. Valle.

Neutrinoless Double beta Decay in SU(2) x U(1) Theories.

Phys. Rev., D25:2951, 1982.

[74] J.J. Sakurai.

Modern Quantum Mechanics.

Addison Wesely Publishing co., Boston, USA, 1994.

[75] Casey R. Watson, John F. Beacom, Hasan Yuksel, and Terry P. Walker.
Direct X-ray Constraints on Sterile Neutrino Warm Dark Matter.
Phys.Rev., D74:033009, 2006.

[76] Herbi K. Dreiner, Howard E. Haber, and Stephen P. Martin.
Two-component spinor techniques and Feynman rules for quantum field theory and supersymmetry.
Phys.Rept., 494:1–196, 2010.

[77] Steven Weinberg.
A Model of Leptons.
Phys.Rev.Lett., 19:1264–1266, 1967.

[78] H. Fritzsch, Murray Gell-Mann, and H. Leutwyler.
Advantages of the Color Octet Gluon Picture.
Phys.Lett., B47:365–368, 1973.

[79] David J. Gross and Frank Wilczek.
Ultraviolet Behavior of Nonabelian Gauge Theories.
Phys.Rev.Lett., 30:1343–1346, 1973.